Journal of Automation and Intelligence 3 (2024) 57–72

Contents lists available at ScienceDirect

Journal of Automation and Intelligence

journal homepage: www.keaipublishing.com/en/journals/journal-of-automation-and-intelligence/

Research article

Actuator and sensor fault isolation in a class of nonlinear dynamical systems ☆

Hamed Tirandaz, Christodoulos Keliris, Marios M. Polycarpou *

KIOS Research Center for Intelligent Systems and Networks, and the Department of Electrical and Computer Engineering, University of Cyprus, Nicosia 1678, Cyprus

ARTICLE INFO

Keywords:
Actuator and sensor fault isolation
Adaptive approximation
Observer-based fault diagnosis
Reasoning-based decision logic

ABSTRACT

Fault isolation in dynamical systems is a challenging task due to modeling uncertainty and measurement noise, interactive effects of multiple faults and fault propagation. This paper proposes a unified approach for isolation of multiple actuator or sensor faults in a class of nonlinear uncertain dynamical systems. Actuator and sensor fault isolation are accomplished in two independent modules, that monitor the system and are able to isolate the potential faulty actuator(s) or sensor(s). For the sensor fault isolation (SFI) case, a module is designed which monitors the system and utilizes an adaptive isolation threshold on the output residuals computed via a nonlinear estimation scheme that allows the isolation of single/multiple faulty sensor(s). For the actuator fault isolation (AFI) case, a second module is designed, which utilizes a learning-based scheme for adaptive approximation of faulty actuator(s) and, based on a reasoning decision logic and suitably designed AFI thresholds, the faulty actuator(s) set can be determined. The effectiveness of the proposed fault isolation approach developed in this paper is demonstrated through a simulation example.

1. Introduction

In recent years, due to the appearance of sophisticated and cyber–physical systems, the task of fault detection, identification of the fault type (sensor/actuator/process) and fault isolation have become a crucial component in ensuring safe system operation and reliability [1–4]. However, despite the major attention the research community placed on fault isolation in dynamical systems, there are still some key challenges in actuator and sensor fault isolation in nonlinear dynamical systems that need to be addressed. These challenges include distinguishing between a fault and the modeling uncertainty and/or measurement noise, determining the type of the fault, dealing with multiple and concurrent faults, isolating the faulty component(s) (which sensor(s) or actuator(s) are faulty), and also, in interconnected systems dealing with the fault propagation problem (i.e., how a fault in one system affects neighboring systems).

For fault diagnosis in nonlinear dynamical systems, observer-based approaches are commonly used, and these are also used in this paper. In this context, there exist two classes of observer-based fault diagnosis approaches in the literature: (i) approaches that utilize a single nonlinear observer [5–7] and, (ii) approaches that utilize a bank of observers [8,9]. Observer-based approaches can also be roughly categorized into reasoning-based [10,11] and, online approximation schemes [12,13]. In observer-based fault diagnosis of dynamical systems, when system residuals are sensitive to a subset of faults (structured residuals), then the use of the fault signature matrix, constitutes an efficient way of isolating multiple faults in such systems [10,11]. However, reasoning-based decision logic fault isolation methods cannot always accurately isolate all faulty components, especially when the distinguishability of faults is difficult to be achieved due to the multiple system components cases (combinations of faulty components) that need to be checked. On the other hand, online approximation schemes (i.e., adaptive approximation, neural networks, etc.) provide a powerful technique for isolating and estimating the faults in nonlinear uncertain systems. The rationale behind these approaches is the online approximation of unmodeled nonlinear faults by using adaptive approximation models [14,15]. The majority of the online approximation-based fault isolation schemes in the literature deal with only one type of fault: either sensor faults [9,16,17], process faults [12,18] or actuator faults [15,19,20]. However, in practice several types of faults are possible. In general, research works that consider several types of faults (usually process and sensor faults) are limited [5,7,13,21–25]. In addition, research works that deal with the isolation of multiple faults and of multiple types are even fewer [13,22,26,27]. In the literature, researchers often impose some restrictions on fault structures to facilitate fault type

Peer review under responsibility of Chongqing University.

☆ This work was co-funded by the European Research Council (ERC) under the ERC Synergy grant agreement No. 951424 (Water-Futures) and by the European Union's Horizon 2020 research and innovation programme under grant agreement No. 739551 (KIOS CoE) and the Government of the Republic of Cyprus through the Directorate General for European Programmes, Coordination and Development.

* Corresponding author.
E-mail addresses: hamedtirandaz@gmail.com (H. Tirandaz), keliris.chris@gmail.com (C. Keliris), mpolycar@ucy.ac.cy (M.M. Polycarpou).

https://doi.org/10.1016/j.jai.2024.03.001
Received 2 November 2023; Received in revised form 24 January 2024; Accepted 13 March 2024
Available online 16 March 2024

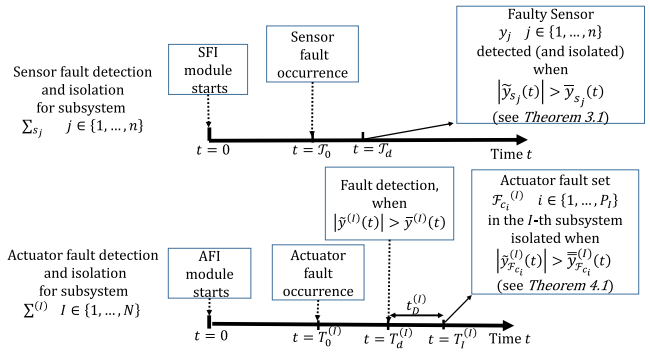

Fig. 1. Diagram describing the procedure of the sensor and actuator fault isolation schemes developed in this paper.

distinguishability. Moreover, these schemes consider the persistence of excitation of fault signals, necessitating fault signals to exhibit sufficient variability over time for precise identification. Nevertheless, accurately distinguishing between sensor and actuator faults becomes challenging, especially in scenarios where fault structures are unrestricted or in the absence of persistency of excitation. Consequently, the limitations of approximation schemes in distinguishing such faulty scenarios highlights the need for of a fault isolation scheme capable of identifying the fault type it is, distinguishing it among the various types it can be, and isolating the faulty component(s) accurately. This work aims to fill this gap.

Motivated by the above discussion, the problem of isolating multiple sensor and actuator fault(s) in nonlinear dynamical systems, is investigated in this research work. Specifically, we consider situations where either (multiple) sensor faults or (multiple) actuator faults occur; hence, the co-existence case of both sensor and actuator faults is not considered in this work. The main goal of this paper is the identification of the fault type and the accurate isolation of the faulty sensor(s) or actuator(s). To this end, actuator and sensor fault isolation are accomplished in two distinct modules that are assigned to monitor the system: (i) the SFI module, and (ii) the AFI module. The SFI module is responsible for isolating the potential faulty sensor(s) in the system, whereas the isolation of actuator fault(s) are determined in the AFI module. In the SFI module, a nonlinear estimation scheme is designed to obtain the isolation thresholds that allows the scheme to isolate accurately and simultaneously multiple abrupt sensor faults in the system. On the other hand, the AFI module contains a fault detection scheme and an adaptive approximation-based actuator fault estimation and isolation scheme to isolate potential actuator fault(s). Fig. 1 shows the overall procedure of the actuator and sensor fault isolation approach proposed in this paper. As shown, both the AFI and the SFI modules are activated at time $t = 0$ s, and monitor independently the system for the presence of faults. In the case of the SFI module, when a fault is detected it is automatically isolated at the same time. It is important to note that the SFI module is sensitive only to sensor faults. Hence, when a single/multiple sensor fault(s) is/are detected (and hence isolated) by the SFI module, then it is guaranteed to be a sensor type fault, so any subsequent fault detection by the AFI module is ignored. Then, any potential faults that are not identified in the SFI module can be regarded as actuator faults. As a result, the proposed scheme in this paper can accurately be utilized for the identification of the fault type. It is worth noting that the designed SFI scheme in this paper exhibits effective performance even in situations where there is a lack of persistence of excitation in fault signals and without prior knowledge of fault signal structures.

In the AFI module, when a fault is detected in a subsystem by the fault detection agent, a bank of estimators (related to the faulty subsystem) are activated to estimate the potential faulty actuators and make a decision about the occurrence of fault(s) on the actuator(s). However, the results of an AFI module of a subsystem will be overridden when at least one sensor is already identified as faulty by the SFI module. The decisions about the possible faults and how these faults can be detected by the AFI and SFI modules are summarized in Table 1. In addition, the structure of the proposed sensor and actuator fault isolation is illustrated in Fig. 2.

Table 1
Actuator and sensor fault isolation cases in this paper.

	SFI module	AFI module
Healthy case	No fault is detected nor isolated.	No fault is detected nor isolated.
Sensor fault(s)	Fault(s) can be detected and isolated (simultaneously at detection).	Fault(s) can be detected by the fault detection agent but the results are overridden by the SFI module results.
Actuator fault(s)	Fault(s) cannot be detected.	Fault(s) can be detected and isolated.

In summary, the key contributions of this paper are:

(i) The identification of the fault type (sensor or actuator) and the accurate isolation of the faulty sensor(s) or actuator(s).
(ii) In the case of faulty sensor(s), a novel reasoning-based FDI scheme is introduced that can accurately identify and isolate the potential faulty sensor(s) within a nonlinear system containing multiple actuators and sensors. Additionally, the proposed scheme can distinguish faulty sensor(s) from actuator(s), and hence, accurate fault type identification can be achieved.
(iii) In the case of faulty actuator(s), an adaptive approximation scheme is developed for approximating and isolating the faulty actuator(s) in each subsystem.
(iv) The proposed actuator and sensor fault isolation scheme is capable of handling various challenges, including modeling uncertainty, measurement noise, interactive effects of multiple faults, and the propagation of faults among subsystems. This versatility is capable of improving the performance of fault isolation in realistic scenarios.

The organization of this paper is as follows: Section 2 contains the mathematical modeling and problem formulation. The structure of the SFI module, containing a modified Luenberger estimator along with an SFI threshold is derived in Section 3 for isolating sensor fault(s). The structure of the AFI module which contains a fault detection and an adaptive approximation-based AFI scheme is presented in Section 4. Simulation results are provided in Section 5 and finally, some concluding remarks are given in Section 6.

Notation: In this paper, $|\cdot|$ indicates the absolute value of a scalar function and the Euclidean 2-norm in the case of vectors. For simplicity, the variables in functions are sometimes omitted if it is clear from the context.

2. Problem formulation

In this paper, we consider a class of dynamical systems given by:

$$\boldsymbol{\Sigma}: \begin{cases} \dot{x}(t) = Ax(t) + Bu_H(t) + Bu_F(t) + g(x(t)) + \eta(x,t) \\ y(t) = x(t) + \xi_y(t) + \beta(t - \mathcal{T}_0) f_y(x,t), \end{cases} \tag{1}$$

where $x \in \mathbb{R}^n$, $u_H \in \mathbb{R}^m$, $u_F \in \mathbb{R}^m$ and $y \in \mathbb{R}^n$ denote the state, the healthy control input, the actuator fault in the control input, and the output vector of the system, respectively. The constant known matrices $A \triangleq [a_{ik}]_{n\times n} \in \mathbb{R}^{n\times n}$ and $B \triangleq [b_{ik}]_{n\times m} \in \mathbb{R}^{n\times m}$ represent the linear part of the system dynamics and $g(x) \triangleq [g_1(x), \dots, g_n(x)]^T : \mathbb{R}^n \to \mathbb{R}^n$ is the known local nonlinear part of the function dynamics of the system and is considered to be a differentiable vector function with respect to variable x. The differentiability of g with respect to x is needed for the design of the adaptive threshold and the stability of

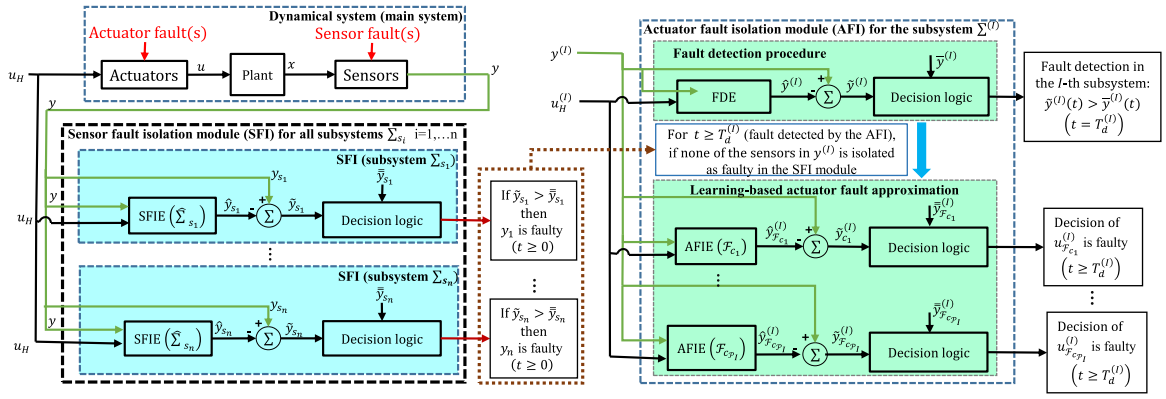

Fig. 2. Actuator and sensor fault isolation modules in this paper.

the estimators designed in this paper. The vector function $\eta(x,t) \triangleq [\eta_1(x,t),\dots,\eta_n(x,t)]^T : \mathbb{R}^n \times \mathbb{R}^+ \to \mathbb{R}^n$ characterizes the unknown modeling uncertainty and disturbances and, $\xi_y(t) \triangleq \left[\xi_{y,1}(t),\dots,\xi_{y,n}(t)\right]^T \in \mathbb{R}^n$ is the (bounded) measurement noise vector. The sensor fault(s) in the system are denoted by $\beta(t-\mathcal{T}_0)f_y(x,t)$, where the function $f_y(x,t) \triangleq [f_{y,1}(x,t),\dots,f_{y,n}(x,t)]^T : \mathbb{R}^n \times \mathbb{R}^+ \to \mathbb{R}^n$ denotes the sensor fault vector in the system, $\beta(t-\mathcal{T}_0) \triangleq diag\left\{\beta_1(t-\mathcal{T}_{0,1}),\dots,\beta_n(t-\mathcal{T}_{0,n})\right\} \in \mathbb{R}^{n\times n}$ where $\beta_i(t-\mathcal{T}_{0,i}) \quad i=1,\dots,n$ is the time profile of the sensor fault occurring in the ith sensor and $\mathcal{T}_0 \triangleq [\mathcal{T}_{0,1},\dots,\mathcal{T}_{0,n}] \in \mathbb{R}^n$ where $\mathcal{T}_{0,i} \quad i=1,\dots,n$ is the unknown time occurrence of the fault in the ith sensor. In this work, we consider only abrupt faults, and therefore the time profile function β_i is given by

$$\beta_i(t-\mathcal{T}_{0,i}) = \begin{cases} 0 & \text{if } t < \mathcal{T}_{0,i} \\ 1 & \text{if } t \geq \mathcal{T}_{0,i} \end{cases} \qquad i=1,\dots,n.$$

Note that sensor faults in Eq. (1) are represented by the vector $\beta(t-\mathcal{T}_0)f_y(x,t)$ which provides distinct fault functions for each sensor along with different fault occurrence time.

For the case of actuator faults, the actuator output u_i (ith element of u) is modeled as follows:

$$u_i(t) = u_{H,i}(t) + u_{F,i}(t) \quad i=1,\dots,m, \tag{2}$$

where $u_{H,i} \in \mathbb{R}$ is the ith element of the healthy actuator outputs u_H; and $u_{F,i}$ is the ith element of the vector function u_F which represents the actuator faults and is defined as follows

$$u_F(t) \triangleq -Y(t-T_0)\Lambda u_H(t), \tag{3}$$

where $Y(t) \triangleq diag\{Y_1(t),\dots,Y_m(t)\}$, $Y_i : \mathbb{R}^+ \to \mathbb{R} \quad i=1,\dots,m$ denotes the unknown time profile function of the fault in the ith actuator of the system. Specifically, in this paper, we consider $Y_i \quad i=1,\dots,m$ as an exponentially decreasing function, modeled as

$$Y_i(t-T_{0,i}) = \begin{cases} 0 & \text{for all } t < T_{0,i} \\ 1-exp(-\delta_i(t-T_{0,i})) & \text{for all } t \geq T_{0,i}, \end{cases}$$

where $\delta_i > 0 \quad i=1,\dots,m$ is the unknown fault evolution rate which affects the time profile Y_i of the ith actuator. Incipient actuator faults result from small values of δ_i whereas abrupt faults in actuator u_i result from larger values of δ_i; $T_{0,i}$ denotes the unknown fault occurrence time in the ith actuator u_i. We consider actuator faults that cause loss of effectiveness on the actuator's performance, which the rate of loss is denoted by the matrix $\Lambda = diag\{\Lambda_1,\dots,\Lambda_{m_I}\}$ where $\Lambda_i \in [0,1]$ indicates the loss of effectiveness of the ith actuator.

Consider the structure of the multi-input multi-output nonlinear dynamical system in this paper which is given in (1), which is susceptible to multiple abrupt sensor faults or actuator faults outlined by various sensors and actuators in the system. The main objectives of sensor and actuator fault isolation scheme presented in this paper can be summarized by two main aspects: (i) identification of fault type (sensor or actuator), and (ii) accurate isolation of the faulty sensor(s) or actuator(s). To achieve these goals, the following assumptions are made.

Assumption 2.1 (*Well-posedness*)**.** The state vector $x(t)$ remains bounded before and after the occurrence of any actuator fault, i.e. $x(t) \in L_\infty \quad \forall t \geq 0$.

The above assumption is required for well-posedness since in this work we deal with the fault isolation problem (not with the feedback control problem), therefore all the signals used for fault isolation have to be bounded. It is worth mentioning that the proposed fault isolation scheme is independent of the control and accommodation task, hence the developed fault isolation algorithms can be combined with existing feedback control and accommodation schemes.

Assumption 2.2. Each element of the unknown modeling uncertainty function η and each element of the measurement noise $\xi_y(t)$ satisfy respectively the following bounding conditions ($\forall t \geq 0$):

$$\left|\eta_i(x,t)\right| \leq \bar{\eta}_i \qquad i=1,\dots,n, \tag{4}$$

and

$$\left|\xi_{y,i}(t)\right| \leq \bar{\xi}_{y,i} \qquad i=1,\dots,n, \tag{5}$$

where $\bar{\eta}_i$ and $\bar{\xi}_{y,i}$ denote known positive constants.

Assumption 2.3. The sensor fault function $f_{y,i}$ and the actuator fault function $u_{F,i}(t)$ for all $i=1,\dots,n$ are bounded, i.e., $|f_{y,i}| < \bar{f}_{y,i}$ and $|u_{F,i}(t)| < \bar{u}_{F,i}$ where the bounds $\bar{f}_{y,i}$ and $\bar{u}_{F,i}$ are sufficiently large known positive constants.

Assumption 2.4. The magnitude of a sensor fault is sufficiently large such that it satisfies ($\forall t \geq \mathcal{T}_{0,i}$):

$$|f_{y,i}| > 4\bar{\xi}_{y,i} \quad i \in \{1,\dots,n\}.$$

Assumption 2.2 is needed to distinguish the effects of the fault from the modeling uncertainty and disturbance noise. This is a common assumption used in the fault diagnosis literature, see [11,28]. Assumption 2.3 is needed for the design of the SFI scheme (specifically for the derivation of isolation thresholds) which will be described later on. It must be noted that the scheme can also handle sensor and actuator faults with unknown bounds, as will be explained in the sequel in Remark 3.2. Furthermore, Assumptions 2.1–2.3 are also required for the stability of the estimators which will be designed in the sequel. Assumption 2.4 indicates the sensor faults that are isolable by the SFI module and is based on the findings of Theorem 3.1(b) in the sequel, such that these faults can be guaranteed to be detected and isolated by the SFI module, the results of which override the results of the AFI. This Assumption essentially eliminates the case of a small sensor fault

not being detected by the SFI, and erroneously being considered as an actuator fault if detected by the AFI module.

Considering the nonlinear dynamical system, which is given in (1) and validity of the Assumptions 2.1 to 2.4, in the subsequent sections, the design of the AFI and the SFI modules are presented in order to achieve the objectives outlined in this paper. The procedure for the developed sensor and actuator fault isolation schemes is depicted in Fig. 1. In summary, the procedures for actuator and sensor fault isolation unfold in the following steps:

1. At time $t = 0$ s, both the SFI module and the fault detection in the AFI module are initiated.
2. If a residual violation occurs in the SFI module, it indicates the accurate isolation of the faulty sensor. It is important to note that, in the SFI module only a sensor fault can lead to the violation of an output residual from its corresponding SFI threshold.
3. If a fault is detected in the AFI module, and if the SFI module does not diagnose a faulty sensor, the AFI estimation procedure is activated to identify faulty actuators.

Fig. 2 illustrates the overall structure of the proposed sensor and actuator fault isolation approach in this paper.

For designing the SFI and AFI modules, a corresponding system decomposition for the dynamical system given (1) will be used, that will lead in a collection of multiple interconnected subsystems. Specifically, for SFI each system state will be considered as a single subsystem, whereas for AFI the decomposition must be made such that each actuator affects only one subsystem (which can be the same among different actuators). Further details for each decomposition process and the designed isolation schemes for isolating faulty actuators and sensors are given in their corresponding sections in the sequel.

3. Sensor fault isolation

3.1. SFI decomposition procedure

In the case of SFI, the system given in (1) is decomposed into n subsystems, one for each system state x_i and its corresponding output y_i. Specifically, the ith subsystem $\Sigma_{s_i} \quad i = 1, \dots, n$ is given by

$$\Sigma_{s_i} : \begin{cases} \dot{x}_i = a_{ii}x_i + A_i\underline{x}_i + B_iu_H + B_iu_F + g_i(x) + \eta_i(x,t) \\ y_i = x_i + \xi_{y,i} + \beta_i(t - \mathcal{T}_{0,i})f_{y,i}(x,t), \end{cases} \tag{6}$$

where a_{ii} is the ith diagonal element of matrix A; A_i and B_i are the ith row of matrices A and B respectively; $x_i \in \mathbb{R}$ and $y_i \in \mathbb{R}$ are the ith elements of state vector x and output vector y respectively and $\underline{x}_i$ is the same vector as x except its ith element which is set to zero, i.e., $\underline{x}_i \triangleq [x_1, \dots, x_{i-1}, 0, x_{i+1}, \dots, x_n]^T$. Since g is considered a differentiable vector function with respect to variable x, then g_i (ith element of g) is Lipschitz with respect to variable x and has Lipschitz constant L_{g_i} which is considered known.

In the following, an example is given to explain the decomposition process applicable for SFI.

Example 1. Consider the following system

$$\Sigma : \begin{cases} \dot{x} = g(x) + Bu \\ y = x + \xi_y + \beta(t - \mathcal{T}_0)f_y(x,t), \end{cases} \tag{7}$$

where $x = [x_1, \dots, x_5]^T \in \mathbb{R}^5$, $u = [u_1, \dots, u_4]^T \in \mathbb{R}^4$ and $y = [y_1, \dots, y_5]^T \in \mathbb{R}^5$ denote the state, actuator control input and output vector of the system, respectively; note that $u = u_H + u_F$; $g = [g_1, \dots, g_5]^T \in \mathbb{R}^5$ where $g_j \quad j = 1, \dots, 5$ are some functions; $\xi_y \in \mathbb{R}^5$ denotes the noise in the system; $\beta(t - \mathcal{T}_0) = diag\{\beta_{1,1}(t - \mathcal{T}_{0,1}), \dots, \beta_{5,5}(t - \mathcal{T}_{0,5})\}$ and $f_y \in \mathbb{R}^5$ are time profile of the fault and sensor fault vector respectively. Assume the matrix coefficient B is given by

$$B = \begin{bmatrix} b_{1,1} & b_{1,2} & 0 & 0 \\ 0 & b_{2,2} & b_{2,3} & 0 \\ 0 & 0 & 0 & b_{3,4} \\ 0 & 0 & 0 & b_{4,4} \\ 0 & 0 & 0 & 0 \end{bmatrix},$$

where $b_{j,k} \quad j,k \in \{1, \dots, 4\}$ denote some actuator coefficients. Then, according to the decomposition given in (6), we obtain the following subsystems that are utilized in the SFI module:

$$\Sigma_{s_i} : \begin{cases} \dot{x}_i = g_i(x) + B_iu \\ y_i = x_i + \xi_{y,i} + \beta_i(t - \mathcal{T}_0)f_y(x,t), \end{cases} \qquad i = 1, \dots, 5,$$

where B_i and β_i are the ith row of matrices B and β respectively. The aforementioned decomposition is depicted in Fig. 3.

3.2. A modified Luenberger estimator design

In general, in interconnected systems, a fault in one subsystem can affect its neighboring subsystem's behavior and this is significant in the case of sensor faults, in which the fault can be propagated among subsystems in many ways [29]. In [28], the authors have proved in their setting that sensor faults under certain conditions can be detected by their corresponding detection agents or by neighboring subsystems detection agents. Besides fault propagation, the effects of the estimator gain matrix on the system residuals are also a challenge in the diagnosability and distinguishability of the faulty sensor(s). Hence, the SFI problem becomes more challenging, because the inspection for sensor faults has to be done beyond the subsystem in which the fault is detected. In the literature, researchers have usually utilized some form of the Luenberger estimator which applies a gain matrix to ensure the stability of the estimation error and estimate the system states. As a result, the effects of the sensor fault propagation in output residuals, are mostly and directly empowered by the estimator gain matrix. Hence, in the proposed SFI design, by properly adjusting the estimator matrix gain, the effects of sensor fault(s) propagation in output residuals can be reduced and thus, it can help reach better sensor fault isolation decisions.

The purpose of this subsection is to design a Luenberger estimator for the main system (1) that has a diagonal gain matrix. In the sequel, a lemma is given for designing a diagonal estimator gain which will be utilized for the design of the SFI module.

Lemma 3.1 ([30]). *Consider the complex square matrix $\Pi \triangleq [\pi_{ij}] \in \mathbb{C}^{n\times n}$ and $\pi_{ii} < 0$ for all $i = 1, \dots, n$. Then, if there exist $\omega \in [0,1]$, $\varphi_i > 0$, and $\varpi_i \leq 1$ for all $i = 1, \dots, n$, such that the following inequalities are satisfied*

$$|\pi_{ii}| > \frac{1}{\varphi_i^{\omega}\varpi_i^{1-\omega}}\Big(\sum_{j=1,j\neq i}^{n}|\pi_{ij}|\varphi_j\Big)^{\omega}\Big(\sum_{j=1,j\neq i}^{n}|\pi_{ji}|\varpi_j\Big)^{1-\omega} \qquad \text{for all } i \in \mathbb{N}_{\omega},$$

and

$$|\pi_{ii}| \geq \frac{R_i(\Pi)^{\omega}C_i(\Pi)^{1-\omega}}{\varphi_i\varpi_i} \qquad \text{for all } i \in \bar{\mathbb{N}}_{\omega},$$

then, matrix Π is Hurwitz, where

$$R_i(\Pi) \triangleq \sum_{j=1,j\neq i}^{n}|\pi_{ij}|, \quad C_i(\Pi) \triangleq \sum_{j=1,j\neq i}^{n}|\pi_{ji}|$$

$\mathbb{N}_{\omega} \triangleq \{j \in \{1, \dots, n\} \,|\, |\pi_{jj}| > R_j(\Pi)^{\omega}C_j(\Pi)^{1-\omega}\}$, *and* $\bar{\mathbb{N}}_{\omega} \triangleq \{j \in \{1, \dots, n\} \,|\, j \notin \mathbb{N}_{\omega}\}$.

In the sequel, using the above lemma, an estimator gain matrix $\mathcal{K}$ is designed which guarantees the stability of the designed estimators in this paper.

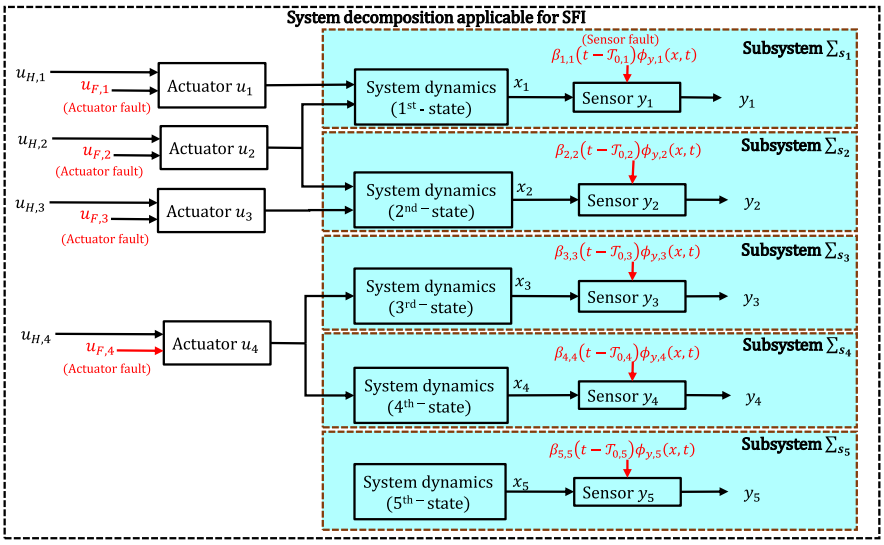

Fig. 3. System decomposition structure applicable for SFI in Example 1 given by (7). Note that all of the states are considered available in all subsystems, i.e., the states x_i for all $i = 1, \dots, n$ are available in all subsystems Σ_{s_i} $i = 1, \dots, n$; furthermore, for simplicity, the subsystems resulting from sensor decomposition are highlighted with light blue color.

Corollary 3.1. *Considering Lemma 3.1, a Luenberger estimator with a diagonal estimator matrix gain $\bar{\mathcal{K}} \triangleq diag\{\bar{\mathcal{K}}_{11}, \dots, \bar{\mathcal{K}}_{nn}\}$ can be designed for the main system (1), such that $A - \bar{\mathcal{K}}$ is Hurwitz, by selecting $\bar{\mathcal{K}}_{ii}$ $i = 1, \dots, n$ to be sufficiently large such that $\bar{\mathcal{K}}_{ii} > a_{ii}$ and $|a_{ii} - \bar{\mathcal{K}}_{ii}| > \sum_{j=1, j\neq i}^{n} |a_{ij}|$.*

Proof. The validity of this Corollary can be easily verified by setting the parameters in the Lemma 3.1 to $\omega_i = 1$, $\varphi_i = 1$, $\varpi_i = 1$ for all $i = 1, \dots, n$, and the matrix $\Pi = A - \bar{\mathcal{K}}$. □

In the sequel, by applying Corollary 3.1 on matrix A of the main system (1), an estimator gain matrix $\mathcal{K}$ and a modified estimator can be obtained which facilitate sensor fault isolation.

Consider the ith subsystem Σ_{s_i} given in (6), and by following the concept of diagonal estimator gain matrix given in Corollary 3.1, we design the following estimator for each subsystem Σ_{s_i} $i = 1, \dots, n$

$$\hat{\Sigma}_{s_i} : \begin{cases} \dot{\hat{x}}_{s_i} = a_{ii}\hat{x}_{s_i} + A_i \underline{y}_{\bar{i}} + B_i u_H \\ \qquad\quad + g_i(\hat{x}_{s_i}, \underline{y}_{\bar{i}}) + \mathcal{K}_{ii}(y_i - \hat{y}_{s_i}) \\ \hat{y}_{s_i} = \hat{x}_{s_i}, \end{cases} \tag{8}$$

where $\hat{x}_{s_i}$ and $\hat{y}_{s_i}$ are the estimation of the state x_i and the corresponding output y_i, respectively. $\underline{y}_{\bar{i}}$ is the same vector as y except its ith element which is set to zero, i.e., $\underline{y}_{\bar{i}} \triangleq [y_1, \dots, y_{i-1}, 0, y_{i+1}, \cdot, y_n]$. $\mathcal{K}_{ii}$ denotes the ith diagonal element of the diagonal matrix $\mathcal{K}$ which is designed such that: (a) $A - \mathcal{K}$ is Hurwitz, by applying Corollary 3.1, and (b) for stability purposes $\mathcal{K}_{ii}$ must also satisfy $\mathcal{K}_{ii} > a_{ii} + L_{g_i}$ $i \in \{1, \dots, n\}$, where L_{g_i} is the Lipschitz constant of the Lipschitz function g_i (ith element of g) which is defined in (6). As a result, the diagonal gain $\mathcal{K}_{ii}$ must be designed such that the following inequalities are satisfied:

$$\mathcal{K}_{ii} > a_{ii} + L_{g_i}, \tag{9a}$$

$$|a_{ii} - \mathcal{K}_{ii}| > \sum_{j=1, j\neq i}^{n} |a_{ij}|. \tag{9b}$$

Note that, by selecting sufficiently large values $\mathcal{K}_{ii}$, conditions (9a) and (9b) are always satisfied. Essentially, this design leads to a high-gain estimator. Additionally, when a larger estimator gain $\mathcal{K}_{ii}$ is selected, the magnitude of the SFI threshold decreases, which is more suitable for the abrupt SFI case, which will be discussed in detail later on, in this section.

It is worth noting that in the state dynamics of the ith sensor isolation estimators $\hat{\Sigma}_{s_i}$ given in (8), without loss of generality, we have considered y_j as the estimation of the $\hat{x}_{s_j}$ for all $j \in \{1, \dots, n\} \backslash i$.

3.3. Reasoning-based sensor fault isolation

In this subsection, the ith subsystem given in (6) through the system Σ decomposition for SFI, along with the modified estimator designed in (8), (9a) and (9b), are utilized to determine the state residual $\tilde{x}_{s_i}$ and its corresponding output residual $\tilde{y}_{s_i}$. Then, the corresponding SFI threshold $\bar{y}_{s_i}$ is designed. Notably, this SFI threshold is tailored to detect faults originating solely from the ith sensor, and therefore when the residual $\tilde{y}_{s_i}$ exceeds its threshold $\bar{y}_{s_i}$ at some time $\mathcal{T}_{0,i}$, it is guaranteed that a sensor fault has occurred in the ith sensor measuring y_i. Therefore, in the case of SFI, the fault detection and isolation occur simultaneously. The procedure for SFI is also depicted in Figs. 1 and 2.

The sensor fault isolation can be realized based on the following theorem. Note that the SFI scheme can achieve the isolation of multiple sensor faults, given that Assumption 2.4 holds (as will be shown by Theorem 3.1(b)), even in the presence of actuator faults. Even though we do not consider the coexistence of sensor and actuator faults, for generality, we provide the following theorem that covers this case as well.

Theorem 3.1. *Considering the ith subsystem Σ_{s_i} given in (6), its estimation $\hat{\Sigma}_{s_i}$ given in (8), with sufficiently large gain $\mathcal{K}_{ii}$ such that inequalities (9a) and (9b) are satisfied and under Assumptions 2.1–2.3, we have:*

(a) if the ith sensor is healthy, i.e., $f_{y,i} = 0$, then the sensor output estimation error $\tilde{y}_{s_i} \triangleq y_i - \hat{y}_{s_i}$ is uniformly bounded and satisfies

$$|\tilde{y}_{s_i}(t)| \leq \bar{y}_{s_i}(t), \tag{10}$$

where

$$\bar{y}_{s_i}(t) \triangleq \bar{x}_{s_i}(t) + \bar{\xi}_{y,i}(t), \tag{11}$$

$$\bar{x}_{s_i}(t) \triangleq C_i(t) + \int_0^t e^{(L_{g_i} + \mathcal{A}_{ii})(t-\tau)} C_i(\tau) d\tau, \tag{12}$$

$$C_i(t) \triangleq e^{\mathcal{A}_{ii} t} \bar{x}_{i,0} + \int_0^t e^{\mathcal{A}_{ii}(t-\tau)} \left[\gamma_i - \mathcal{A}_{ii} \bar{\xi}_{y,i}\right] d\tau, \tag{13}$$

$$\gamma_i \triangleq |B_i| \bar{u}_F + \sum_{j=1, j\neq i}^{n} |a_{ij}| (\bar{\xi}_{y,j} + \bar{f}_{y,j}) + L_{g_i} \sum_{j \in \mathcal{Z}_i} (\bar{\xi}_{y,j} + \bar{f}_{y,j}) + \bar{\eta}_i + a_{ii} \bar{\xi}_{y,i}, \tag{14}$$

where $\mathcal{A}_{ii} \triangleq a_{ii} - \mathcal{K}_{ii}$; $\bar{u}_F \triangleq [\bar{u}_{F,1}, \dots, \bar{u}_{F,m}]^T \in \mathbb{R}^m$, where $\bar{u}_{F,i}$ $i = 1, \dots, m$ is a sufficiently large bound on $u_{F,i}(t)$ (see Assumption 2.3); $\bar{x}_{i,0}$ is a threshold for $\tilde{x}_i(0)$; and $\mathcal{Z}_i = \{j \parallel g_i \text{ is directly affected by state } x_j\}$.

(b) If the ith sensor is healthy, then for any $\epsilon_i > 0$, the estimator gain $\mathcal{K}_{ii}$ can be determined such that the output estimation error $\tilde{y}_{s_i}(t)$ remains bounded by $2\bar{\xi}_{y,i} + \epsilon_i$ for all $t \geq t_{0,i}$, where $t_{0,i} > 0$ denotes a user selectable delay time. In other words, in the absence of fault in the ith sensor, and for any $\epsilon_i > 0$ and $t_{0,i} > 0$, there exists a scalar $\mathcal{M}_{ii} > 0$ such that for all $\mathcal{K}_{ii} \geq \mathcal{M}_{ii}$, the inequality $|\tilde{y}_{s_i}(t)| \leq \bar{y}_{s_i}(t) \leq 2\bar{\xi}_{y,i} + \epsilon_i$ is satisfied for all $t \geq t_{0,i}$.

Proof. *(a)* Considering the system dynamics Σ_{s_i} given in (6) and its estimation $\hat{\Sigma}_{s_i}$ given in (8), the ith residual $\tilde{x}_{s_i} \triangleq x_i - \hat{x}_{s_i}$ of the system under healthy mode of the ith sensor (i.e., $f_{y,i} = 0$), can be written as

$$\begin{cases} \dot{\tilde{x}}_{s_i} = a_{ii}\tilde{x}_{s_i} + A_i(\underline{x}_i - \underline{y}_i) + B_i u_F + g_i(x) \\ \quad -g_i(\hat{x}_{s_i}, \underline{y}_i) + \eta_i(x,t) - \mathcal{K}_{ii}(y_i - \hat{y}_{s_i}) \\ \tilde{y}_{s_i} = \tilde{x}_{s_i} + \xi_{y,i}. \end{cases} \tag{15}$$

Note that in (15), the sensor y_i is considered healthy, but other sensors and also actuators can be faulty (the faults are bounded), see Assumption 2.3. Then, by integrating the state dynamics of (15), we obtain,

$$\tilde{x}_{s_i} = \int_0^t e^{\mathcal{A}_{ii}(t-\tau)}\big(B_i u_F + \sum_{j=1,j\neq i}^{n} a_{ij}(-\xi_{y,j} - f_{y,j}) + g_i(x) \\ - g_i(\hat{x}_{s_i}, \underline{y}_i) + \eta_i(x,\tau) - \mathcal{K}_{ii}(\xi_{y,i})\big)\mathrm{d}\tau + e^{\mathcal{A}_{ii}t}\tilde{x}_i(0). \tag{16}$$

By considering the boundedness of modeling uncertainty η_i, the boundedness of measurement noise $\xi_{y,i}$, and the boundedness of fault function $f_{y,i}$ for all $i = 1,\dots,n$ and $u_{F,i}$ $i = 1,\dots,m$ which are given respectively in Assumptions 2.2–2.3, and also by considering the Lipschitz condition for the function g_i in x, and by using the fact that $|\underline{x}_i - \underline{y}_i| \leq |\underline{x}_{i,1} - \underline{y}_{i,1}| + \cdots + |\underline{x}_{i,n} - \underline{y}_{i,n}|$, (16) can be written by using the triangle inequality as:

$$|\tilde{x}_{s_i}| \leq \int_0^t e^{\mathcal{A}_{ii}(t-\tau)}\Big[|B_i|\bar{u}_F + \sum_{j=1,j\neq i}^{n} |a_{ij}|(\bar{\xi}_{y,j} + \bar{f}_{y,j}) + \bar{\eta}_i \\ + L_{g_i}\big(|\tilde{x}_{s_i}| + \sum_{j\in\mathcal{I}_i}(\bar{\xi}_{y,j} + \bar{f}_{y,j})\big) + \mathcal{K}_{ii}(\bar{\xi}_{y,i})\Big]\mathrm{d}\tau + e^{\mathcal{A}_{ii}t}\bar{x}_{i,0}.$$

Then, by applying the Bellman–Gronwall Lemma [31], we obtain

$$|\tilde{x}_{s_i}(t)| \leq \bar{x}_{s_i}(t),$$

where $\bar{x}_{s_i}(t)$ is defined in (12). As a result, by considering $\tilde{y}_{s_i}(t) = \tilde{x}_{s_i}(t) + \xi_{y,i}(t)$, and by using the triangle inequality, the inequality given in (10) can be obtained.

(b) The solution of (13) is given by

$$C_i(t) = e^{\mathcal{A}_{ii}t}\bar{x}_{i,0} + (1 - e^{\mathcal{A}_{ii}t})(\bar{\xi}_{y,i} - \frac{\gamma_i}{\mathcal{A}_{ii}}),$$

and hence

$$C_i(t) \leq e^{\mathcal{A}_{ii}t}\bar{x}_{i,0} - \frac{\gamma_i}{\mathcal{A}_{ii}} + \bar{\xi}_{y,i}. \tag{17}$$

Therefore, by using the triangle inequality, and after some operations, the state threshold in (12) can be shown to satisfy

$$\bar{x}_{s_i}(t) \leq \Phi_i(t, \mathcal{K}_{ii}), \tag{18}$$

where

$$\Phi_i(t, \mathcal{K}_{ii}) \triangleq \bar{\xi}_{y,i} + \Xi_i(t, \mathcal{K}_{ii}), \tag{19}$$

$$\Xi_i(t, \mathcal{K}_{ii}) \triangleq -\frac{\gamma_i}{\mathcal{A}_{ii}} + \bar{x}_{i,0}\Big(\frac{e^{(\mathcal{A}_{ii}+L_{g_i})t} - e^{\mathcal{A}_{ii}t}}{L_{g_i}}\Big) \\ - \frac{1}{\mathcal{A}_{ii} + L_{g_i}}\Big(\bar{\xi}_{y,i} - \frac{\gamma_i}{\mathcal{A}_{ii}}\Big) + e^{\mathcal{A}_{ii}t}\bar{x}_{i,0} \\ + \frac{e^{(\mathcal{A}_{ii}+L_{g_i})t}}{\mathcal{A}_{ii} + L_{g_i}}(\bar{\xi}_{y,i} - \frac{\gamma_i}{\mathcal{A}_{ii}}). \tag{20}$$

Note that Ξ_i is a monotonically decreasing function with respect to both variables $\mathcal{K}_{ii}$ and time t, i.e., $\frac{\partial \Xi_i}{\partial t} \leq 0$ and $\frac{\partial \Xi_i}{\partial \mathcal{K}_{ii}} \leq 0$ $(\forall t > 0$ and $\forall \mathcal{K}_{ii} > 0)$. Note that considering stability conditions (9a) and (9b), we have $\mathcal{K}_{ii} > 0$. As a result, we have

$$\max_{\forall t \geq t_{0,i}, \forall \mathcal{K}_{ii} \geq \mathcal{M}_{ii}} \Xi_i(t, \mathcal{K}_{ii}) \leq \Xi_i(t, \mathcal{K}_{ii})\Big|_{t=t_{0,i}, \mathcal{K}_{ii}=\mathcal{M}_{ii}}. \tag{21}$$

In addition Ξ_i is a non-negative function, i.e., $\Xi_i(t, \mathcal{K}_{ii}) \geq 0$ for all $t \geq 0$ and for all $\mathcal{K}_{ii}$ that satisfy in (9a) and (9b). Furthermore, for any $t > 0$, we have $\lim_{\mathcal{K}_{ii}\to\infty} \Xi_i(t, \mathcal{K}_{ii}) = 0$. Hence, by considering the Eqs. (10), (11), (18), (19), (20) and (21), and in the absence of a fault in the ith sensor, and for any $\epsilon_i > 0$, and $t_{i,0} > 0$ there exists a scalar $\mathcal{M}_{ii} > 0$ such that for any estimator gain $\mathcal{K}_{ii} \geq \mathcal{M}_{ii}$ that satisfies (9a) and (9b) we have that $\Xi_i(t, \mathcal{K}_{ii}) < \epsilon_i \quad \forall t \geq t_{0,i}$; and as a result $|\tilde{y}_{s_i}(t)| \leq \bar{y}_{s_i}(t) \leq 2\bar{\xi}_{y,i} + \epsilon_i \quad \forall t \geq t_{0,i}$. □

Lemma 3.2. *Based on Theorem 3.1(b), by selecting $\mathcal{K}_{ii} \gg \mathcal{M}_{ii}$, an abrupt sensor fault with magnitude greater than $4\bar{\xi}_{y,i}$ that occurs at time $\mathcal{T}_{0,i}$, i.e., $\left|\beta_i(t - \mathcal{T}_{0,i})f_{y,i}(\mathcal{T}_{0,i})\right| > 4\bar{\xi}_{y,i}$ where $\beta_i(0) = 1$, is guaranteed to be isolated.*

Proof. Based on the proof of Theorem 3.1(b), since Ξ_i is a monotonically decreasing function with respect to $\mathcal{K}_{ii}$, a large value $\mathcal{K}_{ii}$ can diminish ϵ_i, i.e., $\epsilon_i \to 0$ as $\mathcal{K}_{ii} \to \infty$. Therefore, when the estimator gain $\mathcal{K}_{ii}$ in the estimator $\hat{\Sigma}_{s_i}$ in (8), has a large magnitude, i.e., $\mathcal{K}_{ii} \gg \mathcal{M}_{ii}$ (and hence $\epsilon_i \simeq 0$), the sensor noise has large effects on the output (and state) estimation (i.e., $\hat{y}_{s_i} = \hat{x}_{s_i}$ approaches y_i, not x_i), however, the output estimation in the healthy sensor condition lies in the interval $[x_i - \bar{\xi}_{y,i}, x_i + \bar{\xi}_{y,i}]$, i.e., $\hat{y}_{s_i} \in [x_i - \bar{\xi}_{y,i}, x_i + \bar{\xi}_{y,i}]$. Furthermore, in the healthy sensor conditions, from (1), we have $y_i \in [x_i - \bar{\xi}_{y,i}, x_i + \bar{\xi}_{y,i}]$ and since $|y_i - \hat{y}_{s_i}| \leq \bar{y}_{s_i} \leq 2\bar{\xi}_{y,i}$, therefore, sensor faults with magnitude less than $4\bar{\xi}_{y,i}$ may not be isolated. On the other hand, abrupt sensor faults with magnitude greater than $4\bar{\xi}_{y,i}$ are guaranteed to be isolated by utilizing the estimator $\hat{\Sigma}_{s_i}$ and its corresponding isolation threshold. □

Based on Theorem 3.1, if at some time t, the sensor output estimation error $\tilde{y}_{s_i}$ exceeds its threshold $\bar{y}_{s_i}$, i.e., $|\tilde{y}_{s_i}(t)| > \bar{y}_{s_i}(t)$, then it is guaranteed that the ith sensor is faulty.

The sensor fault isolation process is illustrated in Fig. 4 for the subsystem Σ_{s_i} $i \in \{1,\dots,n\}$, in which a potential abrupt fault in sensor y_i is detected and accurately isolated using only the estimator $\hat{\Sigma}_{s_i}$ and its corresponding isolation threshold $\bar{y}_{s_i}$, which is designed in (10)–(14).

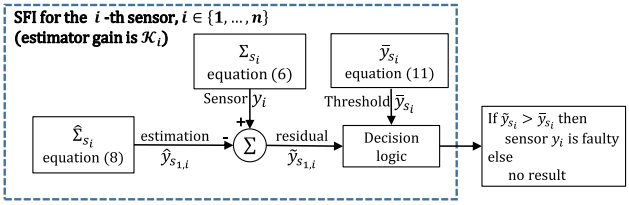

Fig. 4. SFI operation for diagnosis of abrupt sensor fault in sensor y_i.

Remark 3.1. Considering Theorem 3.1(b), in the absence of fault in the ith sensor $i = 1,\dots,n$ (other sensors and actuators can be faulty), for any small $\epsilon_i > 0$, and a given delay time $t_{0,i} > 0$, since $\Xi_i(t, \mathcal{K}_{ii})$ is a strictly decreasing function with respect to both variables $\mathcal{K}_{ii}$ and time t, and also Ξ_i diminishes to zero with respect to $\mathcal{K}_{ii}$, i.e., $\lim_{\mathcal{K}_{ii}\to\infty} \Xi_i(t, \mathcal{K}_{ii}) = 0$, we can define $\mathcal{M}_{ii}$ as:

$$\mathcal{M}_{ii} \triangleq \min\left\{\mathcal{K}_{ii} \;\middle|\; \Xi_i(t_{0,i}, \mathcal{K}_{ii}) < \epsilon_i\right\}. \tag{22}$$

Note that $\mathcal{M}_{ii}$ in (22) can be readily computed by using a binary search algorithm on (20) and then $\mathcal{K}_{ii}$ can be selected such that $\mathcal{K}_{ii} \gg \mathcal{M}_{ii}$.

Remark 3.2. The sensor and actuator fault bounds are required in designing the SFI thresholds $\bar{y}_{s_i}\quad i=1,\dots,n$ (see (10)–(14)) and that is why these bounds are considered to be known in Assumption 2.3. However, it is important to note that, by increasing the estimator gain $\mathcal{K}_{ii}$ the impact of the fault bounds on the SFI thresholds $\bar{y}_{s_i}$ decreases (see the proof of Theorem 3.1(b)). Consequently, the proposed SFI scheme can be effectively applied to systems with unknown fault bounds. To this end, a sufficiently large estimator gain $\mathcal{K}_{ii}\gg\mathcal{M}_{ii}$ can be used which will lead to the isolation threshold having a value $\bar{y}_{s_i}<2\bar{\xi}_{y,i}\quad\forall t\geq t_{0,i}$. Hence, a conservative isolation threshold can be set as $\bar{y}_{s_i}\triangleq 2\bar{\xi}_{y,i}$, which along with a sufficiently large estimator gain $\mathcal{K}_{ii}\gg\mathcal{M}_{ii}$ can provide SFI in systems with unknown fault bounds.

Remark 3.3. In [32,33], a filtering approach to reduce the effects of measurement noise for fault detection was proposed. Hence, the filtering approach in [32,33] can be applied in our settings to mitigate the effect of noise on the abrupt SFI and thus enhance the sensor fault isolability performance.

Remark 3.4. It is important to note that actuator faults cannot be detected by the SFI module simply because, actuator faults cannot trigger the SFI module. Considering the SFI threshold given in (10)–(14) of Theorem 3.1, and the validity of Assumption 2.3 for the boundedness of the sensor and actuator faults, then, in the ith subsystem Σ_{s_i} the only possible violation of the output residual $\tilde{y}_{s_i}\triangleq y_i-\hat{y}_{s_i}\quad i=1,\dots,n$, from its corresponding SFI threshold $\bar{y}_{s_i}$ can be due to the fault in sensor y_i, and not other components in the system. In other words, a bounded fault in actuators and other sensors $y_j\quad j\in\{1,\dots,n\}/i$ cannot cause the violation of the output residual $\tilde{y}_{s_i}$ from its corresponding SFI threshold $\bar{y}_{s_i}$. It is also worth mentioning, that the isolability of the sensor faults can be achieved even in the presence of unknown bounded actuator and/or process faults something that is not considered in this paper, since we do not consider the case of having different fault types coexisting.

Remark 3.5. Considering the Assumption 2.2, which is given for the boundedness of the modeling uncertainty and measurement noise, the designed SFI thresholds given in (10)–(14) of Theorem 3.1 are designed to be robust to both the modeling uncertainty and measurement noise by including the aforementioned bounds. As a result, in the absence of a sensor fault, the residuals $\tilde{y}_{s_i}$ are below their corresponding thresholds $\bar{y}_{s_i}$ thus, guaranteeing no false alarms.

4. Actuator fault isolation

4.1. AFI decomposition procedure

In view of the fact that an actuator can directly affect many state dynamics, the actuator fault isolation cannot be realized by the decomposition of the system given in (6) for SFI. Hence, we consider a different system decomposition for the case of AFI such that the main system in (1) is decomposed in N subsystems $\Sigma^{(I)}\quad I=1,\dots,N$, where the Ith subsystem $\Sigma^{(I)}$ contains a set of actuators $\mathcal{U}^{(I)}$ such that the ith actuator $u_i\quad i\in\{1,\dots,m\}$ appears exclusively in one set and hence in one subsystem, i.e.,

$$u_i\in\mathcal{U}^{(I)}\ \text{iff}\ u_i\notin\mathcal{U}^{(J)},\ \text{for all}\ I,J\in\{1,\dots,N\},I\neq J. \tag{23}$$

Based on the aforementioned actuator partitioning, the state variables and corresponding output variables of system Σ in (1) are assigned to one of the subsystems $\Sigma^{(I)}\quad I=1,\dots,N$. Note that a sensor can appear at maximum in one subsystem (no sensor overlapping in system decomposition; see Fig. 5 for more detail). Hence, the dynamics of the Ith subsystem $\Sigma^{(I)}\quad I=1,\dots,N$ are given by:

$$\Sigma^{(I)}:\begin{cases}\dot{x}^{(I)}=A^{(I)}x^{(I)}+B^{(I)}u^{(I)}+p^{(I)}(x^{(I)})\\ \qquad\qquad +q^{(I)}(x^{(I)},z^{(I)})+\eta^{(I)}(x^{(I)},z^{(I)},t)\\ y^{(I)}=x^{(I)}+\xi_y^{(I)}+\beta^{(I)}(t-\mathcal{T}_0^{(I)})f_y^{(I)}(x^{(I)},t),\end{cases} \tag{24}$$

where $x^{(I)}\in\mathbb{R}^{n_I},u^{(I)}\in\mathbb{R}^{m_I}$ and $y^{(I)}\in\mathbb{R}^{n_I}$ represent respectively the state, the input and the output vectors of the Ith subsystem (note that considering (1) and (2) we have $u^{(I)}\triangleq u_H^{(I)}+u_F^{(I)}$); $z^{(I)}\in\mathbb{R}^{\bar{n}_I}$ represents the set of interconnection variables, i.e., the states of the other subsystems that affect the Ith subsystem; the known matrices $A^{(I)}\in\mathbb{R}^{n_I\times n_I}$ and $B^{(I)}\in\mathbb{R}^{n_I\times m_I}$ represent the local linear part of the subsystem, $p^{(I)}:\mathbb{R}^{n_I}\to\mathbb{R}^{n_I}$ is the known local nonlinear part of the function dynamics of the Ith subsystem, and $q^{(I)}:\mathbb{R}^{n_I}\times\mathbb{R}^{\bar{n}_I}\to\mathbb{R}^{n_I}$ represents the known part of the interconnection function of the Ith subsystem. Note that by considering (1), $p^{(I)}$ and $q^{(I)}$ consist of some terms in g, i.e., $g^{(I)}\triangleq p^{(I)}+q^{(I)}$ and since $g^{(I)}$ is considered differentiable with respect to x, then $p_i^{(I)}$ (ith element of $p^{(I)}$) is Lipschitz with respect to the variable $x^{(I)}$ and has a Lipschitz constant $L_{p_i^{(I)}}$ which is considered known. In addition, $q_i^{(I)}$ (ith element of $q^{(I)}$) is also Lipschitz with known Lipschitz constants $L_{q_i^{(I)}}^{(x)}$ and $L_{q_i^{(I)}}^{(z)}$ with respect to variables $x^{(I)}$ and $z^{(I)}$, respectively for all $i=1,\dots,n_I$. The function $\eta^{(I)}:\mathbb{R}^{n_I}\times\mathbb{R}^{\bar{n}_I}\times\mathbb{R}^{+}\to\mathbb{R}^{n_I}$ is the unknown uncertainty in the Ith subsystem. The sensor fault in the Ith subsystem is denoted by $\beta^{(I)}(t-\mathcal{T}_0^{(I)})f_y^{(I)}(x,t)\in\mathbb{R}^{n_I}$.

Lemma 4.1. *There exists a known constant $L_{q_i^{(I)}}$ such that*

$$|q_i^{(I)}(x^{(I)},z^{(I)})-q_i^{(I)}(\hat{x}^{(I)},y_z^{(I)})|\leq L_{q_i^{(I)}}(|x^{(I)}-\hat{x}^{(I)}|+\bar{\xi}_z^{(I)})$$
$$\forall\, x^{(I)},\hat{x}^{(I)}\in\mathcal{X},z^{(I)},y_z^{(I)}\in Z,\quad i=1,\dots,n_I,$$

where $\bar{\xi}_z^{(I)}$ is a bound on $\xi_z^{(I)}\triangleq y_z^{(I)}-z^{(I)}$, (where $y_z^{(I)}$ denotes the output vector associated with $z(t)$, i.e. $y_z^{(I)}=z^{(I)}+\xi_z^{(I)}$) i.e., $|\xi_z^{(I)}|\leq\bar{\xi}_z^{(I)}$; and $L_{q_i^{(I)}}\triangleq\max\{L_{q_i^{(I)}}^{(x)},L_{q_i^{(I)}}^{(z)}\}$.

Proof. Since $q_i^{(I)}$ is considered Lipschitz in variables $x^{(I)}$ and $z^{(I)}$, the proof is straightforward and is therefore omitted (it is based on the Lipschitz conditions on each variable and the triangle inequality). □

It can be easily shown that the vector functions $p^{(I)}$ and $q^{(I)}$ that contain the scalar Lipschitz functions $p_i^{(I)}$ and $q_i^{(I)}$ are Lipschitz, with Lipschitz constants $L_{p^{(I)}}\triangleq\left(\sum_{i=1}^{n_I}(L_{p_i^{(I)}})^2\right)^{\frac{1}{2}}$ and $L_{q^{(I)}}\triangleq\left(\sum_{i=1}^{n_I}(L_{q_i^{(I)}})^2\right)^{\frac{1}{2}}$ respectively.

Example 2. We apply the above actuator decomposition process for the system example provided in Eq. (7) to demonstrate how the subsystems are considered in the case of AFI. This will lead to the following decomposition, which will be utilized in the AFI module to isolate the faulty actuators:

$$\text{Subsystem}\ \Sigma^{(1)}:\begin{cases}\dot{x}^{(1)}=g^{(1)}(x^{(1)},z^{(1)})+B^{(1)}u^{(1)}\\ y^{(1)}=x^{(1)}+\xi_y^{(1)}+\beta^{(1)}(t-\mathcal{T}_0^{(1)})f_y^{(1)},\end{cases}$$

and

$$\text{Subsystem}\ \Sigma^{(2)}:\begin{cases}\dot{x}^{(2)}=g^{(2)}(x^{(2)},z^{(2)})+B^{(2)}u^{(2)}\\ y^{(2)}=x^{(2)}+\xi_y^{(2)}+\beta^{(2)}(t-\mathcal{T}_0^{(2)})f_y^{(2)},\end{cases}$$

where $x^{(1)}=[x_1,x_2]^T$, $u^{(1)}=[u_1,u_2,u_3]^T$, and $y^{(1)}=[y_1,y_2]^T$ denote the state, input and output vector of subsystem $\Sigma^{(1)}$; $x^{(2)}=[x_3,x_4,x_5]^T$, $u^{(2)}=[u_4]^T$, $y^{(2)}=[y_3,y_4,y_5]^T$ are the state, input and output vector of subsystem $\Sigma^{(2)}$; $g^{(1)}=[g_1,g_2]^T$, $g^{(2)}=[g_3,g_4,g_5]^T$, $\xi_y^{(1)}=[\xi_{y,1},\xi_{y,2}]^T$, $\xi_y^{(2)}=[\xi_{y,3},\xi_{y,4},\xi_{y,5}]^T$, $f_y^{(1)}=[f_{y,1},f_{y,2}]^T$ and $f_y^{(2)}=[f_{y,3},f_{y,4},f_{y,5}]^T$; $B^{(1)}$ and $\beta^{(1)}$ consist of the first two rows of the matrices B and β respectively; $B^{(2)}$ and $\beta^{(2)}$ consist of the last three rows of the matrices B and β respectively. Note that in the AFI decomposition process, without loss of generality, the state dynamics $\dot{x}_5$ beside its corresponding output y_5, can be assigned to both subsystems $\Sigma^{(1)}$ and $\Sigma^{(2)}$. The structure of the described decomposition applicable for AFI for the system (7) is depicted in Fig. 5.

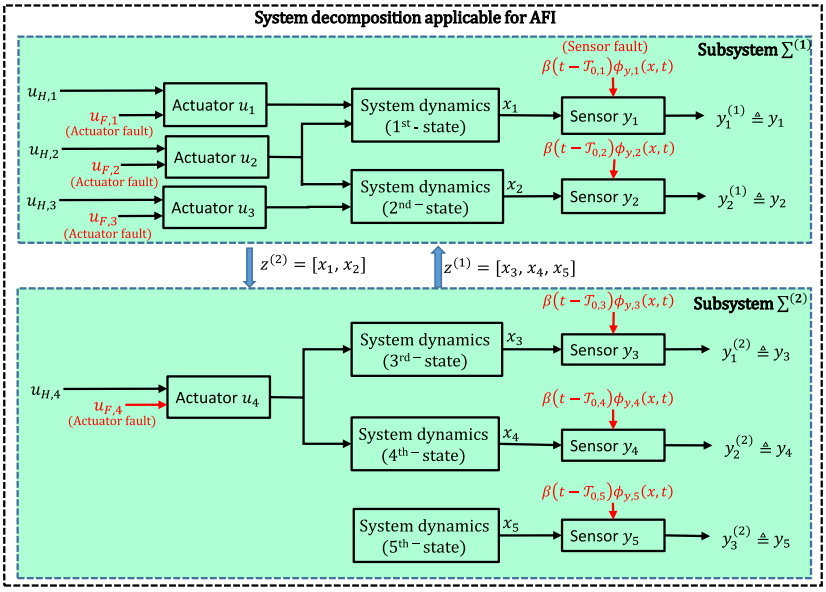

Fig. 5. System decomposition structure applicable for AFI in Example 2 (note that all of the states are considered available in all subsystems, i.e., the states x_i for all $i = 1, \dots, n$ are available in all subsystems $\Sigma^{(I)}$ $I = 1, \dots, M$; furthermore, for simplicity, the subsystems resulting from the actuator decomposition are highlighted with light green color.

4.2. Fault detection procedure

Fault detection is a fundamental and prerequisite task for AFI (see Fig. 2). After a fault is detected in the AFI module, the adaptive approximation-based actuator fault estimation will be activated. Considering the Ith subsystem given in 24, its estimation is given as follows

$$\hat{\Sigma}^{(I)}: \begin{cases} \dot{\hat{x}}^{(I)} = A^{(I)}\hat{x}^{(I)} + B^{(I)}u_H^{(I)} + p^{(I)}(\hat{x}^{(I)}) \\ \qquad\qquad +q^{(I)}(\hat{x}^{(I)}, y_z^{(I)}) + K^{(I)}(y^{(I)} - \hat{y}^{(I)}) \\ \hat{y}^{(I)} = \hat{x}^{(I)}, \end{cases} \tag{25}$$

where $\hat{x}^{(I)}$ and $\hat{y}^{(I)}$ are the estimation of the state vector $x^{(I)}$ and output vector $y^{(I)}$, respectively; $K^{(I)}$ is designed such that $A_k^{(I)} \triangleq A^{(I)} - K^{(I)}$ is diagonal and Hurwitz, i.e., $A_k^{(I)} = diag\{a_{k,1}^{(I)}, \dots, a_{k,n_I}^{(I)}\}$; and also for stability purposes, the elements $a_{k,i}^{(I)}$ are selected such that $a_{k,i}^{(I)} < -L_i^{(I)}$ where $L_i^{(I)} = L_{p_i^{(I)}} + L_{q_i^{(I)}}$ for all $i = 1, \dots, n_I$.

Then, a suitable fault detection threshold, which guarantees the boundedness of the residual $\tilde{y}^{(I)} \triangleq y^{(I)} - \hat{y}^{(I)}$ under the healthy mode of operation is given as follows:

Lemma 4.2 ([34]). *In the healthy conditions and under the Assumptions 2.1–2.2, and by considering the constants $\rho^{(I)}$ and $\nu^{(I)}$ such that $|e^{A_k^{(I)}t}| \leq \rho e^{-\nu^{(I)}t}$ and $\bar{\nu}^{(I)} \triangleq \nu^{(I)} - \rho^{(I)}L^{(I)}$, the output estimation error $\tilde{y}^{(I)} \triangleq y^{(I)} - \hat{y}^{(I)}$ is uniformly bounded and satisfies*

$$|\tilde{y}^{(I)}(t)| \leq \bar{y}^{(I)}(t) \qquad \forall\, t < T_0^{(I)}, \tag{26}$$

and

$$\bar{y}^{(I)}(t) \triangleq \bar{x}^{(I)}(t) + \bar{\xi}_y^{(I)},$$

$$\bar{x}^{(I)}(t) \triangleq q^{(I)}(t) + \rho^{(I)}L^{(I)}\int_0^t e^{-\bar{\nu}^{(I)}(t-s)}\chi^{(I)}(s)\mathrm{d}s, \tag{27}$$

$$\chi^{(I)}(t) \triangleq \rho^{(I)}\int_0^t e^{-\nu^{(I)}(t-\tau)}\psi^{(I)}\mathrm{d}\tau + \rho^{(I)}e^{-\nu^{(I)}t}x_0^{(I)},$$

where $\bar{y}^{(I)}$ denotes the actuator fault detection threshold corresponding to the Ith subsystem; $\bar{\xi}_y^{(I)}$ is a bound on measurement noise $\xi_y^{(I)}$ defined in (5), $x_0^{(I)}$ is a bound on $\left|\tilde{x}^{(I)}(0)\right|$, i.e., $\left|\tilde{x}^{(I)}(0)\right| \leq x_0^{(I)}$, and

$$\psi^{(I)} \triangleq L_{q^{(I)}}\bar{\xi}_z^{(I)} + \bar{\eta}^{(I)} + |K^{(I)}\bar{\xi}_y^{(I)}|.$$

Then, by applying a fault detection scheme on the Ith subsystem 24 and by using its estimation which is given in (25), the local fault detection time $T_d^{(I)}$ for the Ith subsystem is defined as

$$T_d^{(I)} \triangleq \inf\left\{t \,\middle|\, |\tilde{y}^{(I)}(t)| > \bar{y}^{(I)}(t)\right\}.$$

When a fault is detected at some time $T_d^{(I)}$ in the Ith subsystem (when $|\tilde{y}^{(I)}| > \bar{y}^{(I)}$ at $t = T_d^{(I)}$), its corresponding actuator fault approximation estimator is activated to isolate the possible actual faulty actuator(s) set among all actuator(s) of the Ith subsystem, by estimating the faulty actuator(s) magnitude and, implicitly, the loss of the actuator's performance. However, since only one type of faults (either faulty actuator(s) or faulty sensor(s)) is considered in this paper, when some sensors of the subsystem $\Sigma^{(I)}$ are identified as faulty by their SFI modules, then the result of the AFI modules at any time will be overridden, since it is guaranteed that sensor fault(s) have occurred.

4.3. Adaptive approximation-based actuator fault estimation and isolation

In the previous subsection, the Ith subsystem, given in 24, which is obtained through the system $\boldsymbol{\Sigma}$ decomposition for AFI is utilized in conjunction with its corresponding estimator designed in (25) in the fault detection agent of the Ith AFI module to detect the fault(s) in the Ith subsystem. A fault is detected when the residual $\tilde{y}^{(I)}$ exceeds its corresponding threshold $\bar{y}^{(I)}(t)$ which is designed in (26)–(27). It is worth noting that the fault detection agent in the I-AFI module is sensitive to both potential sensor and actuator faults in the system. However, as mentioned earlier, potential sensor faults satisfying Assumption 2.4, i.e., $|f_{y,i}| > 4\bar{\xi}_{y,i}$ will be isolated by their corresponding SFI module, hence, are overridden in the AFI module. As a result, in the AFI module, when a fault is detected by its fault detection agent, the designed adaptive approximation scheme is activated to estimate and isolate the faulty actuators. This activation occurs under the condition that no faulty sensor occurs. To achieve AFI, in this subsection an adaptive approximation-based actuator fault estimation and isolation

scheme is designed that can effectively isolate the faulty actuators in each subsystem. The procedure for the AFI is also depicted in Figs. 1 and 2.

Adaptive approximation, is recognized as a powerful technique for approximating unknown nonlinearity in dynamical systems in real time and has been widely utilized in many research areas such as in estimating modeling uncertainty, adaptive control design and fault estimation. Furthermore, it has been extensively applied for both diagnosing and controlling the behavior of dynamical systems, e.g., [13,14,16,17,35,36]. In the context of AFI, the main fault isolation challenge lies in actuator redundancy (multiple actuators affecting a state dynamic), which affects the isolability of faulty actuators in cases where interactive effects of faults exist. Motivated by this challenge, this paper utilizes adaptive approximation as an inclusive-based logic to systematically explore and identify all potential sets of faulty actuators.

It is worth mentioning that, in fault isolation based on adaptive approximation methods, a set of residuals is usually utilized [35]. In this work, a bank of $\mathcal{P}_I$ estimators $\hat{\Sigma}^{(I)}_{\mathcal{F}_{r_I}}$ $r_I = 1, \dots, \mathcal{P}_I$ are utilized to isolate the actuator fault set in each subsystem $\Sigma^{(I)}$ $I = 1, \dots, N$. In the case of single actuator fault isolation in $\Sigma^{(I)}$, m_I estimators are needed, i.e., $\mathcal{P}_I = m_I$ (note that m_I is the number of actuators in the subsystem $\Sigma^{(I)}$); whereas in the case of multiple actuator fault isolation in $\Sigma^{(I)}$, $2^{m_I} - 1$ estimators are needed, i.e., $\mathcal{P}_I = 2^{m_I} - 1$. It is worth noting that the introduced system decomposition for AFI in this paper minimizes the number m_I of actuators per subsystem. Note that when more than one actuators directly affect a state dynamic, combinatorial effects of actuators appear which make the actuator fault distinguishability more challenging. For instance, if 3 actuators directly affect a state variable, then there are 7 combinations of potentially faulty sets (assuming there is at least one faulty actuator).

By applying the decomposition process, which is given in Section 4.1, the proposed scheme in this paper utilizes a small number of adaptive estimators and is effective even in cases involving non-distinguishable faulty actuators. Nevertheless, it is important to note that considering the non-distinguishability of faulty actuators in systems with interactive effects of actuators, the isolated actuator set(s) may not be unique. This challenge is addressed in [37], where a stringent assumption is made to restrict the number of actuators in each state dynamic, allowing for a maximum of one actuator in each state dynamic and hence, accurate isolability of faulty actuators can be achieved. In such cases, a reasoning-based fault isolation scheme can effectively isolate the fault(s) detected as a result of a faulty actuator(s). It is worth mentioning that by applying our designed scheme for such cases, specifically in the absence of combinatorial effects of the actuator fault(s), only one estimator $\hat{\Sigma}^{(I)}_{\mathcal{F}}$ is enough to estimate the faulty actuator vector u, where $\mathcal{F}^{(I)} = \{u^{(I)}_1, \dots, u^{(I)}_{m_I}\}$. Hence, in the absence of actuator redundancy, the adaptive approximation-based AFI scheme designed in this paper is capable of distinguishing the faulty actuator set. Nevertheless, in scenarios involving actuator redundancy, implementing multiple estimators of the designed scheme allows for enhanced identification of the potential faulty actuator sets and estimation of the corresponding fault magnitudes. The adaptability of the proposed approximation scheme to the presence of redundant actuators in a system highlights its versatility in improving actuator fault identification and estimation, thereby making a substantial contribution to the overall reliability of the system.

The r_Ith adaptive estimator $\hat{\Sigma}^{(I)}_{\mathcal{F}_{r_I}}$ aims to estimate the Ith subsystem $\Sigma^{(I)}$ in 24 by considering the actuator set $\mathcal{F}^{(I)}_{r_I}$ as faulty and the rest of the actuators as healthy. Therefore, in the r_Ith adaptive estimator $\hat{\Sigma}^{(I)}_{\mathcal{F}_{r_I}}$, the actuator set $\mathcal{F}^{(I)}_{r_I}$ is estimated, where the actuator vector of the r_Ith estimator, i.e., $u^{(I)}_{\mathcal{F}_{r_I}} = [u^{(I)}_{\mathcal{F}_{r_I},1}, \dots, u^{(I)}_{\mathcal{F}_{r_I},m_I}] \in \mathbb{R}^{m_I}$ is such that

$$u^{(I)}_{\mathcal{F}_{r_I},i} = \begin{cases} u^{(I)}_i & \text{if } u^{(I)}_i \in \mathcal{F}^{(I)}_{r_I} \\ 0 & \text{if } u^{(I)}_i \notin \mathcal{F}^{(I)}_{r_I} \end{cases} \qquad i = 1, \dots, m_I.$$

In other words, the vector $u^{(I)}_{\mathcal{F}_{r_I}}$ only contains the potential faulty actuator set $\mathcal{F}^{(I)}_{r_I}$ that will be estimated by $\hat{\Sigma}^{(I)}_{\mathcal{F}_{r_I}}$ and the rest of the elements, that is the actuators that are considered healthy, are zero. Then, the r_Ith adaptive estimator $\hat{\Sigma}^{(I)}_{\mathcal{F}_{r_I}}$ $r_I = 1, \dots, \mathcal{P}_I$ can be designed based on the main subsystem architecture given in 24, as follows:

$$\hat{\Sigma}^{(I)}_{\mathcal{F}_{r_I}} : \begin{cases} \dot{\hat{x}}^{(I)}_{\mathcal{F}_{r_I}} = A^{(I)}\hat{x}^{(I)}_{\mathcal{F}_{r_I}} + B^{(I)}(\hat{u}^{(I)}_{\mathcal{F}_{r_I}} + \bar{\hat{u}}^{(I)}_{\mathcal{F}_{r_I}}) + p(\hat{x}^{(I)}_{\mathcal{F}_{r_I}}) \\ \qquad\qquad + q^{(I)}(\hat{x}^{(I)}_{\mathcal{F}_{r_I}}, y^{(I)}_z) + K^{(I)}(y^{(I)} - \hat{y}^{(I)}_{\mathcal{F}_{r_I}}) + \Omega^{(I)}_{\mathcal{F}_{r_I}}\dot{\bar{\hat{u}}}^{(I)}_{\mathcal{F}_{r_I}} \\ \hat{y}^{(I)}_{\mathcal{F}_{r_I}}(t) = \hat{x}^{(I)}_{\mathcal{F}_{r_I}}(t) \\ \dot{\Omega}^{(I)}_{\mathcal{F}_{r_I}} = A^{(I)}_k \Omega^{(I)}_{\mathcal{F}_{r_I}} + B^{(I)}_{\mathcal{F}_{r_I}} \\ \dot{\hat{u}}^{(I)}_{\mathcal{F}_{r_I}} = \mathcal{P}\{\Gamma^{(I)}_{\mathcal{F}_{r_I}}(\Omega^{(I)}_{\mathcal{F}_{r_I}})^T D^{(I)}[\tilde{y}^{(I)}_{\mathcal{F}_{r_I}}]\}, \end{cases} \tag{28}$$

where $\hat{x}^{(I)}_{\mathcal{F}_{r_I}} \in \mathbb{R}^{n_I}$, $\hat{u}^{(I)}_{\mathcal{F}_{r_I}} \in \mathbb{R}^{m_I}$ and $\hat{y}^{(I)}_{\mathcal{F}_{r_I}} \in \mathbb{R}^{n_I}$ are the estimations of the state vector $x^{(I)}$, the actuator vector $u^{(I)}_{\mathcal{F}_{r_I}}$, and the output vector $y^{(I)}$, respectively for all $r_I = 1, \dots, \mathcal{P}_I$; $\tilde{y}^{(I)}_{\mathcal{F}_{r_I}} \triangleq y^{(I)} - \hat{y}^{(I)}_{\mathcal{F}_{r_I}}$ represents the output estimation error of the r_Ith adaptive estimator; the matrix $K^{(I)} \in \mathbb{R}^{n_I \times n_I}$ is a constant matrix of estimator gains chosen such that $A^{(I)}_k \triangleq A^{(I)} - K^{(I)}$ is diagonal and Hurwitz (designed similarly as in fault detection); $\bar{u}^{(I)}_{\mathcal{F}_{r_I}}$ is the complementary vector of $u^{(I)}_{\mathcal{F}_{r_I}}$ with respect to the actuator vector $u^{(I)}$, i.e., $\bar{u}^{(I)}_{\mathcal{F}_{r_I}} \triangleq u^{(I)} - u^{(I)}_{\mathcal{F}_{r_I}}$ and also, $\bar{\hat{u}}^{(I)}_{\mathcal{F}_{r_I}}$ is the estimation of $\bar{u}^{(I)}_{\mathcal{F}_{r_I}}$. It is worth noting that in the r_Ith estimator, $\bar{\hat{u}}^{(I)}_{\mathcal{F}_{r_I}}$ is considered as healthy, i.e., $\bar{\hat{u}}^{(I)}_{\mathcal{F}_{r_I}} \triangleq \bar{u}^{(I)}_{H,\mathcal{F}_{r_I}}$, where $\bar{u}^{(I)}_{H,\mathcal{F}_{r_I}}$ denotes the healthy values of actuator vector $\bar{u}^{(I)}_{\mathcal{F}_{r_I}}$, however, this may not be true in reality since, $\bar{u}^{(I)}_{\mathcal{F}_{r_I}}$ may contain some faulty actuators. This mismatch is what allows the actuator fault isolation. $\Omega^{(I)}_{\mathcal{F}_{r_I}} \in \mathbb{R}^{n_I \times m_I}$ is the intermediate variable representing the filtered version of $B^{(I)}_{\mathcal{F}_{r_I}}$, where $B^{(I)}_{\mathcal{F}_{r_I}}$ is the same as the matrix $B^{(I)}$ except the matrix column elements in $B^{(I)}$ that do not correspond to any actuators in the set $\mathcal{F}^{(I)}_{r_I}$ (therefore set to zero). In other words, $B^{(I)}_{\mathcal{F}_{r_I}} = \left[b^{(I)}_{\mathcal{F}_{r_I}(ik)}\right]_{n_I \times m_I}$ where

$$b^{(I)}_{\mathcal{F}_{r_I}(ik)} \triangleq \begin{cases} b^{(I)}_{ik} & \text{if } u^{(I)}_k \in \mathcal{F}^{(I)}_{r_I} \\ 0 & \text{if } u^{(I)}_k \notin \mathcal{F}^{(I)}_{r_I} \end{cases} \qquad \begin{array}{l} \text{for all } i = 1, \dots, n_I, \\ \text{and } k = 1, \dots, m_I, \end{array}$$

the matrix $\Gamma^{(I)}_{\mathcal{F}_{r_I}} > 0$ is the learning rate for actuator estimation and $\mathcal{P}$ denotes the projection operator which restricts the actuator estimation within the predefined and convex region set $\Theta^{(I)}_{\mathcal{F}_{r_I}} \in \mathbb{R}^{n_I}$ [38] and also guarantees the stability of the learning algorithm in the presence of the modeling uncertainty and measurement noise. In this paper, $\Theta^{(I)}_{\mathcal{F}_{r_I}}$ is chosen to be a hypersphere of radius $\mathcal{R}^{(I)}_{\mathcal{F}_{r_I}}$. Then, according to [39], the adaptive law for the estimation of $\hat{u}^{(I)}_{\mathcal{F}_{r_I}}$ can be expressed as follows

$$\dot{\hat{u}}^{(I)}_{\mathcal{F}_{r_I}} = \Gamma^{(I)}_{\mathcal{F}_{r_I}}(\Omega^{(I)}_{\mathcal{F}_{r_I}})^T D[\tilde{y}^{(I)}_{\mathcal{F}_{r_I}}] - \mathcal{X}^{(I)}_{\mathcal{F}_{r_I}} \Gamma^{(I)}_{\mathcal{F}_{r_I}} \frac{\hat{u}^{(I)}_{\mathcal{F}_{r_I}} \hat{u}^{(I)T}_{\mathcal{F}_{r_I}}}{\hat{u}^{(I)}_{\mathcal{F}_{r_I}} \Gamma^{(I)}_{\mathcal{F}_{r_I}} \hat{u}^{(I)}_{\mathcal{F}_{r_I}}} \mathcal{P}^{(I)}, \tag{29}$$

where $\mathcal{P}^{(I)} \triangleq \Gamma^{(I)}_{\mathcal{F}_{r_I}}(\Omega^{(I)}_{\mathcal{F}_{r_I}})^T D[\tilde{y}^{(I)}_{\mathcal{F}_{r_I}}]$ and $\mathcal{X}^{(I)}_{\mathcal{F}_{r_I}}$ denotes the indicator function:

$$\mathcal{X}^{(I)}_{\mathcal{F}_{r_I}} = \begin{cases} 0 & \text{if } \{|\hat{u}^{(I)}_{\mathcal{F}_{r_I}}| < \mathcal{R}^{(I)}_{\mathcal{F}_{r_I}}\} \\ & \text{or } \{|\hat{u}^{(I)}_{\mathcal{F}_{r_I}}| = \mathcal{R}^{(I)}_{\mathcal{F}_{r_I}} \text{ and } \hat{u}^{(I)T}_{\mathcal{F}_{r_I}} \mathcal{P}^{(I)} \le 0\} \\ 1 & \text{if } \{|\hat{u}^{(I)}_{\mathcal{F}_{r_I}}| = \mathcal{R}^{(I)}_{\mathcal{F}_{r_I}} \text{ and } \hat{u}^{(I)T}_{\mathcal{F}_{r_I}} \mathcal{P}^{(I)} > 0\}, \end{cases} \tag{30}$$

and $D^{(I)}$ denotes the dead-zone operator:

$$D^{(I)}[\tilde{y}^{(I)}_{\mathcal{F}_{k_I}}] = \begin{cases} 0 & \text{for all } t < T_d^{(I)} \\ \tilde{y}^{(I)}_{\mathcal{F}_{k_I}} & \text{for all } t \geq T_d^{(I)}. \end{cases}$$

In the sequel, the stability and approximation capabilities of the designed adaptive estimator given in (28) are analyzed and demonstrate the ability of the adaptive approximation scheme to isolate the faulty actuators set $\mathcal{F}^{(I)}_{k_I}$ by estimating the loss of performance of the actuators.

Theorem 4.1. *When the actuator fault set $\mathcal{F}^{(I)}_{k_I}$ occurs at time $T_0^{(I)}$, and the fault is detected at time $T_d^{(I)}$, then, provided Assumptions 2.1–2.2 hold, the k_Ith estimator $\hat{\Sigma}^{(I)}_{\mathcal{F}_{k_I}}$ given in (28) that estimates the subsystem $\Sigma^{(I)}$ given in 24 based on the estimation of the actual fault actuator set $\mathcal{F}^{(I)}_{k_I}$ is such that its corresponding residual $\tilde{y}^{(I)}_{\mathcal{F}_{k_I}}$ is bounded, component-wise as $|\tilde{y}^{(I)}_{\mathcal{F}_{k_I},i}(t)| \leq \bar{\tilde{y}}^{(I)}_{\mathcal{F}_{k_I},i}(t)$ for all $i = 1, \ldots, n_I$ for all $t \geq T_d^{(I)} + t_D^{(I)}$ where $t_D^{(I)} > 0$ is a designer selectable parameter (the isolation delay time) and the isolation threshold $\bar{\tilde{y}}^{(I)}_{\mathcal{F}_{k_I}}$ is given by*

$$\bar{\tilde{y}}^{(I)}_{\mathcal{F}_{k_I}}(t) \triangleq \bar{\tilde{x}}^{(I)}_{\mathcal{F}_{k_I}}(t) + \bar{\xi}^{(I)}_y(t) \quad \forall t \geq T_d^{(I)} + t_D^{(I)}, \tag{31}$$

where

$$\bar{\tilde{x}}^{(I)}_{\mathcal{F}_{k_I},i}(t) \triangleq \mathbb{E}^{(I)}_{\mathcal{F}_{k_I},i}(t) + L_i^{(I)} \int_{T_d^{(I)}}^{t} e^{(a^{(I)}_{k,i} + L_i^{(I)})(t-\tau)} \mathbb{E}^{(I)}_{\mathcal{F}_{k_I},i}(\tau) \mathrm{d}\tau,$$

$$\mathbb{E}^{(I)}_{\mathcal{F}_{k_I},i}(t) \triangleq \left| \Omega^{(I)}_{\mathcal{F}_{k_I},i} \right| \kappa^{(I)}_{\mathcal{F}_{k_I}} + \int_{T_d^{(I)}}^{t} e^{a^{(I)}_{k,i}(t-\tau)} \mu^{(I)}_{\mathcal{F}_{k_I},i} \mathrm{d}\tau + e^{a^{(I)}_{k,i}(t-T_d^{(I)})} \bar{x}^{(I)}_{d,i},$$

$$\mu^{(I)}_{\mathcal{F}_{k_I},i} \triangleq L_i^{(I)} \sum_{j=1, j\neq i}^{n_I} \bar{\tilde{x}}^{(I)}_{\mathcal{F}_{k_I},j} + L_{q_i^{(I)}} \bar{\xi}^{(I)}_z + \left| K_i^{(I)} \right| \bar{\tilde{\xi}}^{(I)}_y + |\Omega^{(I)}_{\mathcal{F}_{k_I},i}| \, u^{(I)}_{max}(t_D^{(I)} + T_d^{(I)}) + \bar{\eta}_i^{(I)},$$

where $L_i^{(I)} \triangleq L_{p_i^{(I)}} + L_{q_i^{(I)}}$; $u^{(I)}_{max}$ is an upper-bound on the actuator time derivative $\dot{u}_j \quad j = 1, \ldots, m$, and is given by

$$|\dot{u}_j^{(I)}(t)| < u^{(I)}_{max,j}(T_d^{(I)} + t_D^{(I)}) \quad \forall t \geq T_d^{(I)} + t_D^{(I)}, \tag{32}$$

where

$$u^{(I)}_{max,j}(T_d^{(I)} + t_D^{(I)}) \triangleq (t_D^{(I)} e)^{-1} u^{(I)}_{H,j}(T_d^{(I)} + t_D^{(I)}). \tag{33}$$

$\kappa^{(I)}_{\mathcal{F}_{k_I}}$ is the actuator approximation bound which depends on the geometric properties of the set $\Theta^{(I)}_{\mathcal{F}_{k_I}}$ and is defined as follows for all $t \geq 0$:

$$\kappa^{(I)}_{\mathcal{F}_{k_I}}(t) \triangleq \inf_{\hat{u}^{(I)}_{\mathcal{F}_{k_I}}(t) \in \Theta^{(I)}_{\mathcal{F}_{k_I}}} \left\{ \bar{\kappa}(t) \left| \left| u^{(I)}_{\mathcal{F}_{k_I}}(t) - \hat{u}^{(I)}_{\mathcal{F}_{k_I}}(t) \right| \leq \bar{\kappa}(t) \right. \right\}.$$

Proof. Using the Ith subsystem $\Sigma^{(I)}$ given in 24 and the k_Ith estimator $\hat{\Sigma}^{(I)}_{\mathcal{F}_{k_I}}$ given in (28), that is designed to estimate the fault in the actuator(s) set $\mathcal{F}^{(I)}_{k_I}$, after the detection of the fault caused by the actual faulty actuator(s) set $\mathcal{F}^{(I)}_{k_I}$ at time $T_d^{(I)}$, the state error dynamics of the k_Ith estimator $\dot{\tilde{x}}^{(I)}_{\mathcal{F}_{k_I}} \triangleq \dot{x}^{(I)} - \dot{\hat{x}}^{(I)}_{\mathcal{F}_{k_I}}$ satisfies

$$\begin{aligned} \dot{\tilde{x}}^{(I)}_{\mathcal{F}_{k_I}} &= A^{(I)} x^{(I)} + B^{(I)} u^{(I)} + p^{(I)}(x^{(I)}) + q^{(I)}(x^{(I)}, z^{(I)}) \\ &\quad + \eta^{(I)}(x^{(I)}, z^{(I)}, t) - \Big[A^{(I)} \hat{x}^{(I)}_{\mathcal{F}_{k_I}} + B^{(I)}(\hat{u}^{(I)}_{\mathcal{F}_{k_I}} + \hat{\bar{u}}^{(I)}_{\mathcal{F}_{k_I}}) + p^{(I)}(\hat{x}^{(I)}_{\mathcal{F}_{k_I}}) \\ &\quad + q^{(I)}(\hat{x}^{(I)}_{\mathcal{F}_{k_I}}, y^{(I)}_z) + K^{(I)}(y^{(I)} - \hat{y}^{(I)}_{\mathcal{F}_{k_I}}) + \Omega^{(I)}_{\mathcal{F}_{k_I}} \dot{\hat{u}}^{(I)}_{\mathcal{F}_{k_I}} \Big], \end{aligned} \tag{34}$$

where in the k_Ith estimator the actuator set $\mathcal{F}^{(I)}_{k_I}$ is considered as faulty actuator set and the rest of actuators are considered as healthy, i.e., in the k_Ith estimator, we set $\hat{\bar{u}}^{(I)}_{\mathcal{F}_{k_I}} \triangleq \bar{u}^{(I)}_{H,\mathcal{F}_{k_I}}$. Note that, in the k_Ith estimator, we have $\bar{u}^{(I)}_{\mathcal{F}_{k_I}} \triangleq \bar{u}^{(I)}_{H,\mathcal{F}_{k_I}}$. Hence, (34) becomes

$$\begin{aligned} \dot{\tilde{x}}^{(I)}_{\mathcal{F}_{k_I}} &= A_k^{(I)} \tilde{x}^{(I)}_{\mathcal{F}_{k_I}} + B^{(I)} u^{(I)}_{\mathcal{F}_{k_I}} + \bar{p}^{(I)} + \bar{q}^{(I)} + \eta^{(I)}(x^{(I)}, z^{(I)}, t) \\ &\quad - \left[B^{(I)} \hat{u}^{(I)}_{\mathcal{F}_{k_I}} + K^{(I)} \xi^{(I)}_y + \Omega^{(I)}_{\mathcal{F}_{k_I}} \dot{\hat{u}}^{(I)}_{\mathcal{F}_{k_I}} \right], \end{aligned} \tag{35}$$

where

$$\bar{p}^{(I)} = p^{(I)}(x^{(I)}) - p^{(I)}(\hat{x}^{(I)}_{\mathcal{F}_{k_I}}),$$
$$\bar{q}^{(I)} = q^{(I)}(x^{(I)}, z^{(I)}) - q^{(I)}(\hat{x}^{(I)}_{\mathcal{F}_{k_I}}, y^{(I)}_z).$$

By substituting $B^{(I)}_{\mathcal{F}_{k_I}} = \dot{\Omega}^{(I)}_{\mathcal{F}_{k_I}} - A_k^{(I)} \Omega^{(I)}_{\mathcal{F}_{k_I}}$ from (28) into (35), and considering $\tilde{u}^{(I)}_{\mathcal{F}_{k_I}} \triangleq u^{(I)}_{\mathcal{F}_{k_I}} - \hat{u}^{(I)}_{\mathcal{F}_{k_I}}$, we obtain (note that $B^{(I)}_{\mathcal{F}_{k_I}} \hat{u}^{(I)}_{\mathcal{F}_{k_I}} = B^{(I)} \hat{u}^{(I)}_{\mathcal{F}_{k_I}}$)

$$\begin{aligned} \dot{\tilde{x}}^{(I)}_{\mathcal{F}_{k_I}} &= A_k^{(I)} \tilde{x}^{(I)}_{\mathcal{F}_{k_I}} + \bar{p}^{(I)} + \bar{q}^{(I)} + \eta^{(I)}(x^{(I)}, z^{(I)}, t) \\ &\quad + \left[\dot{\Omega}^{(I)}_{\mathcal{F}_{k_I}} - A_k^{(I)} \Omega^{(I)}_{\mathcal{F}_{k_I}} \right] \tilde{u}^{(I)}_{\mathcal{F}_{k_I}} - K^{(I)} \xi^{(I)}_y - \Omega^{(I)}_{\mathcal{F}_{k_I}} \dot{\hat{u}}^{(I)}_{\mathcal{F}_{k_I}}, \end{aligned}$$

then, we have

$$\begin{aligned} \dot{\tilde{x}}^{(I)}_{\mathcal{F}_{k_I}} &= A_k^{(I)} (\tilde{x}^{(I)}_{\mathcal{F}_{k_I}} - \Omega^{(I)}_{\mathcal{F}_{k_I}} \tilde{u}^{(I)}_{\mathcal{F}_{k_I}}) + \bar{p}^{(I)} + \bar{q}^{(I)} + \eta^{(I)}(x^{(I)}, z^{(I)}, t) \\ &\quad - K^{(I)} \xi^{(I)}_y + d/dt(\Omega^{(I)}_{\mathcal{F}_{k_I}} \tilde{u}^{(I)}_{\mathcal{F}_{k_I}}) - \Omega^{(I)}_{\mathcal{F}_{k_I}} \dot{u}^{(I)}_{\mathcal{F}_{k_I}}. \end{aligned} \tag{36}$$

Let $\varepsilon^{(I)}_{\mathcal{F}_{k_I}} \triangleq \tilde{x}^{(I)}_{\mathcal{F}_{k_I}} - \Omega^{(I)}_{\mathcal{F}_{k_I}} \tilde{u}^{(I)}_{\mathcal{F}_{k_I}}$. Then, (36) can be rewritten as

$$\begin{aligned} \dot{\varepsilon}^{(I)}_{\mathcal{F}_{k_I}} &= A_k^{(I)} \varepsilon^{(I)}_{\mathcal{F}_{k_I}} + \bar{p}^{(I)} + \bar{q}^{(I)} + \eta^{(I)}(x^{(I)}, z^{(I)}, t) - K^{(I)} \xi^{(I)}_y \\ &\quad - \Omega^{(I)}_{\mathcal{F}_{k_I}} \dot{u}^{(I)}_{\mathcal{F}_{k_I}}. \end{aligned} \tag{37}$$

By solving Eq. (37), we have (note that $\Omega^{(I)}_{\mathcal{F}_{k_I}}(T_d^{(I)}) = 0_{n_I \times m_I}$)

$$\begin{aligned} \tilde{x}^{(I)}_{\mathcal{F}_{k_I}} &= \Omega^{(I)}_{\mathcal{F}_{k_I}}(t) \tilde{u}^{(I)}_{\mathcal{F}_{k_I}}(t) + e^{A_k^{(I)}(t-T_d^{(I)})} \tilde{x}^{(I)}_{\mathcal{F}_{k_I}}(T_d^{(I)}) \\ &\quad + \int_{T_d^{(I)}}^{t} e^{A_k^{(I)}(t-\tau)} \left[\bar{p}^{(I)} + \bar{q}^{(I)} - K^{(I)} \xi^{(I)}_y \right. \\ &\quad \left. - \Omega^{(I)}_{\mathcal{F}_{k_I}} \dot{u}^{(I)}_{\mathcal{F}_{k_I}} + \eta^{(I)}(x^{(I)}, z^{(I)}, \tau) \right] \mathrm{d}\tau, \end{aligned} \tag{38}$$

the ith component of $\tilde{x}^{(I)}_{\mathcal{F}_{k_I}}$ in (38) satisfies (note that $A_k^{(I)}$ is a diagonal matrix)

$$\begin{aligned} \tilde{x}^{(I)}_{\mathcal{F}_{k_I},i} &= \Omega^{(I)}_{\mathcal{F}_{k_I},i}(t) \tilde{u}^{(I)}_{\mathcal{F}_{k_I}}(t) + e^{a^{(I)}_{k,i}(t-T_d^{(I)})} \tilde{x}^{(I)}_{\mathcal{F}_{k_I},i}(T_d^{(I)}) \\ &\quad + \int_{T_d^{(I)}}^{t} e^{a^{(I)}_{k,i}(t-\tau)} \left[\bar{p}^{(I)} + \bar{q}^{(I)} - K_i^{(I)} \xi^{(I)}_y \right. \\ &\quad \left. - \Omega^{(I)}_{\mathcal{F}_{k_I},i} \dot{u}^{(I)}_{\mathcal{F}_{k_I}} + \eta_i^{(I)}(x^{(I)}, z^{(I)}, \tau) \right] \mathrm{d}\tau, \end{aligned} \tag{39}$$

where $K_i^{(I)}$ and $\Omega^{(I)}_{\mathcal{F}_{k_I},i}$ are the ith row of matrices $K^{(I)}$ and $\Omega^{(I)}_{\mathcal{F}_{k_I}}$, respectively. By applying the initial condition $\hat{x}^{(I)}_{\mathcal{F}_{k_I},i}(T_d^{(I)}) \triangleq y_i^{(I)}(T_d^{(I)})$, we have $|\tilde{x}^{(I)}_{\mathcal{F}_{k_I},i}(T_d^{(I)})| = |x_i^{(I)}(T_d^{(I)}) - \hat{x}^{(I)}_{\mathcal{F}_{k_I},i}(T_d^{(I)})| = |x_i^{(I)}(T_d^{(I)}) - y_i^{(I)}(T_d^{(I)})| = \xi^{(I)}_{y,i} \leq \bar{x}^{(I)}_{d,i}$, where $\bar{x}^{(I)}_{d,i}$ is a suitable bound for the region of the state operation. Then, based on the Lipschitz condition for the functions $p^{(I)}$ and $q^{(I)}$, the inequality given in (4) of Assumption 2.2 and by using Lemma 4.1, Eq. (39) can be written by using the triangle inequality as:

$$\begin{aligned} \left| \tilde{x}^{(I)}_{\mathcal{F}_{k_I},i} \right| &\leq |\Omega^{(I)}_{\mathcal{F}_{k_I},i}(t) \tilde{u}^{(I)}_{\mathcal{F}_{k_I}}(t)| + e^{a^{(I)}_{k,i}(t-T_d^{(I)})} \bar{x}^{(I)}_{d,i} \\ &\quad + \int_{T_d^{(I)}}^{t} e^{a^{(I)}_{k,i}(t-\tau)} \left[L_i^{(I)} |\tilde{x}^{(I)}_{\mathcal{F}_{k_I}}| + L_{q_i^{(I)}} \bar{\xi}^{(I)}_z \right. \\ &\quad \left. + |K_i^{(I)}| \, |\bar{\tilde{\xi}}^{(I)}_y| + |\Omega^{(I)}_{\mathcal{F}_{k_I},i}| \, |\dot{u}^{(I)}_{\mathcal{F}_{k_I}}| + \bar{\eta}_i^{(I)} \right] \mathrm{d}\tau, \end{aligned}$$

then considering

$$\mathcal{E}_{ik_I}^{(I)}(t) = |\Omega_{F_{k_I},i}^{(I)}(t)\tilde{u}_{F_{k_I}}^{(I)}(t)| + e^{a_{k,i}^{(I)}(t-T_d^{(I)})}\bar{x}_{d,i}^{(I)} + \int_{T_d^{(I)}}^{t} e^{a_{k,i}^{(I)}(t-\tau)}\left[L_{q_i^{(I)}}\bar{\xi}_z^{(I)} + |K_i^{(I)}|\,|\bar{\xi}_y^{(I)}| + |\Omega_{F_{k_I},i}^{(I)}|\,|\dot{u}_{F_{k_I}}^{(I)}| + \bar{\eta}_i^{(I)}\right]\mathrm{d}\tau,$$

we have

$$\left|\tilde{x}_{F_{k_I},i}^{(I)}\right| \le \mathcal{E}_{ik_I}^{(I)}(t) + L_i^{(I)}\int_{T_d^{(I)}}^{t} e^{a_{k,i}^{(I)}(t-\tau)}|\tilde{x}_{F_{k_I}}^{(I)}|\mathrm{d}\tau. \tag{40}$$

Furthermore, since the state estimation error is $\tilde{x}_{F_{k_I}}^{(I)} \triangleq [\tilde{x}_{F_{k_I},1}^{(I)},\dots,\tilde{x}_{F_{k_I},n_I}^{(I)}]$, and by using the fact that $|\tilde{x}_{F_{k_I}}^{(I)}| \le |\tilde{x}_{F_{k_I},1}^{(I)}| + \cdots + |\tilde{x}_{F_{k_I},n_I}^{(I)}|$, (which holds for every norm space), therefore, (40) becomes:

$$|\tilde{x}_{F_{k_I},i}^{(I)}| \le \mathcal{E}_{ik_I}^{(I)} + L_i^{(I)}\int_{T_d^{(I)}}^{t} e^{a_{k,i}^{(I)}(t-\tau)}\Big(|\tilde{x}_{F_{k_I},i}^{(I)}| + \sum_{r=1,r\neq i}^{n_I}|\tilde{x}_{F_{k_I},r}^{(I)}|\Big)\mathrm{d}\tau. \tag{41}$$

Considering

$$E_{ik_I}^{(I)}(t) = \mathcal{E}_{ik_I}^{(I)}(t) + L_i^{(I)}\int_{T_d^{(I)}}^{t} e^{a_{k,i}^{(I)}(t-\tau)}\Big(\sum_{r=1,r\neq i}^{n_I}\left|\tilde{x}_{F_{k_I},r}^{(I)}\right|\Big)\mathrm{d}\tau,$$

and by applying the Bellman–Gronwall Lemma [31], we have

$$|\tilde{x}_{F_{k_I},i}^{(I)}| \le E_{k_I}^{(I)}(t) + L_i^{(I)}\int_{T_d^{(I)}}^{t} e^{(a_{k,i}^{(I)}+L_i^{(I)})(t-\tau)}E_{k_I}^{(I)}(\tau)\mathrm{d}\tau. \tag{42}$$

However, the upper bound in (42) cannot be directly used in fault isolation threshold because it depends on actuator fault approximation error $\tilde{u}_{F_{k_I}}^{(I)}$ and the derivative of faulty actuators $\dot{u}_{F_{k_I}}^{(I)}$. Since the actuator fault approximation $\hat{u}_{F_{k_I}}^{(I)}$ belongs to the known compact set $\Theta_{F_{k_I}}^{(I)}$, then $|u_{F_{k_I}}^{(I)} - \hat{u}_{F_{k_I}}^{(I)}| \le \kappa_{F_{k_I}}^{(I)}(t)$ for a suitable threshold $\kappa_{F_{k_I}}^{(I)}(t)$ which is depends on the geometric properties of the set $\Theta_{F_{k_I}}^{(I)}$. In this paper $\Theta_{F_{k_I}}^{(I)}$ is considered as a hypersphere. Hence, we can select $\kappa_{F_{k_I}}^{(I)}(t) = \mathcal{R}_{F_{k_I}}^{(I)} + |\hat{u}_{F_{k_I}}^{(I)} - O_{F_{k_I}}^{(I)}|$ where $\mathcal{R}_{F_{k_I}}^{(I)}$ and $O_{F_{k_I}}^{(I)}$ represents the radius and the center of the hypersphere $\Theta_{F_{k_I}}^{(I)}$, respectively; another term, $|\dot{u}_{F_{k_I}}^{(I)}(t)|$ is also a challenge. In this paper, we have considered $u_{H,i}^{(I)}$ to be constant for all $i = 1,\dots,m_I$. Then, from (2) we have

$$\dot{u}_i^{(I)}(t) = -\delta_i^{(I)}e^{-\delta_i^{(I)}(t-T_{0,i}^{(I)})}\Lambda_i^{(I)}u_{H,i}^{(I)}(t) \quad \forall t > T_{0,i}^{(I)}, \tag{43}$$

where $\delta_i^{(I)} \in L_\infty$. $\dot{u}_i^{(I)}(t)$ $i = 1,\dots,m_I$ is not bounded and $\dot{u}_i^{(I)}(t)$ can have a large value in a small neighborhood of fault occurrence time $T_{0,i}^{(I)}$. However, considering the actuator fault type in this paper as given in (2), due to the boundedness of the actuator value, the absolute value of the term $\dot{u}_i^{(I)}(t)$ decreases exponentially to zero. Hence, by considering an isolation delay time $t_D^{(I)}$, from (43) we have

$$|\dot{u}_i^{(I)}(t)| \le \delta_i^{(I)}e^{-\delta_i^{(I)}(t_D^{(I)})}u_{H,i}^{(I)}(t) \quad \forall t > T_{d,i}^{(I)} + t_D^{(I)}.$$

Then, it can easily be calculated that the maximum value of $|\dot{u}_i^{(I)}(t)|$, after the isolation delay time $t_D^{(I)}$, will occur at $\delta_i^{(I)} = 1/t_D^{(I)}$ and will be satisfied in (33). As a result, the AFI threshold given in (31) for the k_I th adaptive approximation estimator can be concluded. □

Remark 4.1. Considering (31), (33), and the actuator fault structure considered in this paper which is given in (3), the isolation delay time $t_D^{(I)}$ has to be selected by the designer large enough such that $u_{max,i}^{(I)}$ in (33) and, as a result the AFI threshold in $\bar{\bar{y}}_{F_{k_I}}^{(I)}(t)$ in (31), have small values. Note that when a fault is detected at time $T_d^{(I)}$, then the isolation results will be provided at a time $t \ge T_d^{(I)} + t_D^{(I)}$. It is worth noting that regarding the actuator fault(s) structure considered in this paper, the magnitude of actuator faults $u_{F,i}$ $i = 1,\dots,m$ considered in this paper, as defined in (3) have an exponentially decreasing magnitude with respect to time, and their boundedness is established within the interval $[0, u_{H,i}]$, i.e., $0 \le u_{F,i} \le u_{H,i}$ where $u_{H,i}$ indicates the healthy actuator signal. Given these characteristics, by selecting a small delay time $t_D^{(I)}$ (e.g., a few seconds) is sufficient for evaluating the AFI threshold in Eq. (31). It must be noted though that by opting for a larger delay time $t_D^{(I)}$ leads to a smaller AFI threshold at the mere cost of having increased isolation time. Therefore, the selection of $t_D^{(I)}$ creates a trade off between isolation time and isolation sensitivity.

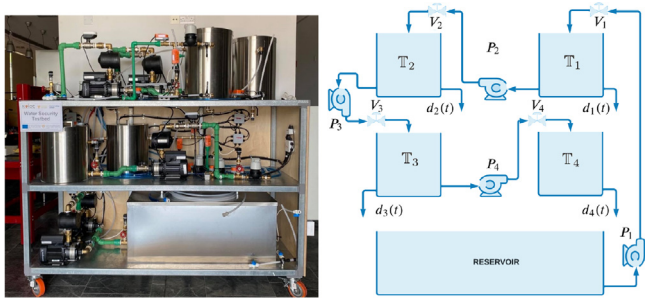

Fig. 6. The KIOS Water Systems Testbed; and a simplified illustration of the series configuration of the KIOS testbed given in [40], where P_I corresponds to the Ith pump and V_I corresponds to the Ith valve, $I = 1,2,3,4$.

Remark 4.2. Consider the adaptive approximation estimator given in (28) along with all possible faulty actuators sets $\mathcal{F}_{r_I}^{(I)}$ for all $r_I = 1,\dots,\mathcal{P}_I$, with actuators approximations given by $\hat{u}_{F_{\bar{I}}}^{(I)}$ (see (29)). Then, the actual fault set $F_{k_I}^{(I)}$ can be isolated by utilizing the designed AFI threshold (31) in Theorem 4.1. However, due to the existence of actuators with weak effects on a subsystem, and also the combinatorial effect of actuators (caused by multiple actuators in the system, like for instance the example given earlier where 3 actuators directly affect a state variable), the isolation fault set may not be unique. This essentially means that there is no guarantee that all but one residuals $\tilde{y}_{F_{\bar{I}},i}^{(I)}(t)$ will remain bounded by its corresponding threshold $\bar{\bar{y}}_{F_{\bar{I}},i}^{(I)}(t)$ $\forall i = 1,\dots,n_I$ and hence the actual faulty set $F_{k_I}^{(I)}$ may not precisely be determined.

5. Simulation

The simulations are performed on the WaterSafe Testbed, a small-scale replica of a water transport network constructed using industrial components and devices, while the communications are implemented in a way that resembles a water utility Supervisory Control and Data Acquisition (SCADA) system. The WaterSafe Testbed has been developed at the KIOS Research and Innovation Center of Excellence at the University of Cyprus, to support the advancement of smart water networks research. The KIOS WaterSafe system and its equivalent block diagram of the water for the configuration is provided in Fig. 6 (see also [40]). In this paper, all valves operate between 0% to 100%, indicating the valve being completely closed and open, respectively. Each tank has a level sensor installed for measuring the water level inside the tank. All pipes of the system have flow control electronic valves, as well as manual valves. It is assumed that the pipes are always filled with water. Further explanations of KIOS WaterSafe Testbed are provided in [40].

The structure of the WaterSafe Testbed system can be dynamically represented as follows,

$$\mathbf{\Sigma}: \begin{cases} \dot{\mathcal{L}}_I(t) = \frac{1}{S_I}\left[\mathcal{Q}_I(t) - \mathcal{Q}_{I+1}(t) - d_I(t)\right] \\ \dot{\mathcal{Q}}_I(t) = \Psi_A\left(\mathcal{Q}_I(t), u_I(t)\right) \end{cases} \quad I = 1,2,3,4, \tag{44}$$

where $\mathcal{L}_I(t)$ and $\mathcal{Q}_I(t)$ are respectively the water level and inflow rate of tank $\mathbb{T}_I$ $I = 1,2,3,4$ at time t (note that $\mathcal{Q}_{I+1}(t)$ denotes the outflow

rate of tank $\mathbb{T}_I$). All states are considered available with measurement sensors (affected by noise), which can be faulty; S_I denotes the tank base area of tank $\mathbb{T}_I \quad I = 1,2,3,4$; $d_I(t) \quad I = 1,2,3,4$ denotes the water consumption which can be modeled using Bernoulli's flow equation for incompressible fluids. The outflow rate from the orifice at the bottom of each tank is given by

$$d_I(t) = \gamma_I(t)\sqrt{2\mathcal{G}\mathcal{L}_I(t)}, \quad I = 1,2,3,4,$$

where $\mathcal{G}$ is the gravitational constant and $\gamma_I(t)$ denotes the cross-section area opening of the consumption outflow pipe at tank $\mathbb{T}_I$ which in real water distribution network is usually unknown. The cross-section opening is controlled by defining the settings of the consumption valve. In this work, the valve opening $\gamma_I(t)$ is considered an unknown disturbance to the system and exhibits periodic behavior.

The WaterSafe Testbed system given in (44) can be represented in the same form as the main system (1) considered in this paper, by defining the state vector $x \in \mathbb{R}^8$ of the system as $x \triangleq \left[\mathcal{L}_1, \mathcal{Q}_1, \mathcal{L}_2, \mathcal{Q}_2, \mathcal{L}_3, \mathcal{Q}_3, \mathcal{L}_4, \mathcal{Q}_4\right]^T$. Then, the state measurements are given by

$$y_i = x_i + \xi_{y,i} + \beta(t - \mathcal{T}_i) f_{y,i}(x,t) \quad i = 1,2,3,4,$$

the matrix $A = diag\left\{0, -\alpha_1, 0, -\alpha_2, 0, -\alpha_3, 0, -\alpha_4\right\} \in \mathbb{R}^{8\times 8}$,

$$B = \begin{bmatrix} 0 & \lambda_1 & 0 & 0 & 0 & 0 & 0 & 0 \\ 0 & 0 & 0 & \lambda_2 & 0 & 0 & 0 & 0 \\ 0 & 0 & 0 & 0 & 0 & \lambda_3 & 0 & 0 \\ 0 & 0 & 0 & 0 & 0 & 0 & 0 & \lambda_4 \end{bmatrix}^T,$$

the control vector $u \in \mathbb{R}^4$ is given by $u = \left[u_1, u_2, u_3, u_4\right]^T$; $g(x,t) = [\frac{1}{S_1}(x_2 - x_4), 0, \frac{1}{S_2}(x_4 - x_6), 0, \frac{1}{S_3}(x_6 - x_8), 0, \frac{1}{S_4}x_8, 0]^T \in \mathbb{R}^8$ is the known local nonlinear part of the function dynamics of the system; $\xi = \left[\xi_{y,1}, \ldots, \xi_{y,8}\right]^T \in \mathbb{R}^8$ is the measurement noise vector and $\eta = [-\frac{d_1}{S_1}, 0, -\frac{d_2}{S_2}, 0, -\frac{d_3}{S_3}, 0, -\frac{d_4}{S_4}, 0]^T : \mathbb{R}^+ \to \mathbb{R}^8$ is the modeling uncertainty and disturbances of the system.

System decomposition procedure

In this part, the AFI and SFI decomposition procedures of the WaterSafe Testbed system presented in (44) are given in detail.

(a) AFI decomposition procedure

By utilizing the criteria given in (23) for the AFI decomposition, the WaterSafe dynamical system in (1) can be decomposed into four distinct and interconnected subsystems $\Sigma^{(I)} \quad I = 1,2,3,4$ based on 24 as follows

$$\Sigma^{(I)} : \begin{cases} \dot{x}_1^{(I)} = \frac{1}{S_I}\left[x_2^{(I)} + q^{(I)}(x^{(I)}, z^{(I)}) - d_I\right] \\ \dot{x}_2^{(I)} = \Psi_A^{(I)}(x_2^{(I)}, u_I) \\ y_i^{(I)} = x_i^{(I)} + \xi_{y,i}^{(I)} + \beta_i^{(I)}(t - \mathcal{T}_{0,i}^{(I)}) f_{y,i}^{(I)}(x^{(I)}, t) \end{cases}$$
$$i = 1,2, \ I = 1,2,3,4, \tag{45}$$

where the change in the state of the tank level $\mathcal{L}_I(t) \quad I = 1,2,3,4$ is denoted respectively by $x_1^{(I)} \quad I = 1,2,3,4$. In addition, the change in the state of the pump $\mathcal{Q}_I(t) \quad I = 1,2,3,4$ is denoted respectively by $x_2^{(I)} \quad I = 1,2,3,4$, and is regulated by the Local Feedback Controller (LFC) in such a way that

$$\Psi_A^{(I)}(x_2^{(I)}, u_I) \triangleq \begin{cases} \lambda_I u_I - \alpha_I x_2^{(I)} & 0.1 < u_I \le 1 \\ -\vartheta_I x_2^{(I)} & 0 \le u_I \le 0.1, \end{cases} \tag{46}$$

which denotes that the pressure typically drops when the pump is 'OFF', resulting in the gradual decrease of the flow. The interconnection terms are $q^{(1)}(x^{(1)}, z^{(1)}) = [-\frac{1}{S_1}x_2^{(2)}, 0]^T$, $q^{(2)}(x^{(2)}, z^{(2)}) = [-\frac{1}{S_2}x_2^{(3)}, 0]^T$, $q^{(3)}(x^{(3)}, z^{(3)}) = [-\frac{1}{S_3}x_2^{(4)}, 0]^T$, and $q^{(4)}(x^{(4)}, z^{(4)}) = [0,0]^T$. Furthermore, considering the defined function $g^{(I)} = p^{(I)} + q^{(I)}$ in (25), we set $p^{(I)} = [0, 0]^T \quad I = 1,2,3,4$. The linear part of the Ith subsystem is $A^{(I)} = [0, \frac{1}{S_I} \ ; \ 0, -\alpha_I]$. The uncertainty term $\eta^{(I)}$ for each subsystem $\Sigma^{(I)} \quad I = 1,2,3,4$ is $\eta^{(1)} = [\frac{d_1}{S_1}, 0]^T$, $\eta^{(2)} = [\frac{d_2}{S_2}, 0]^T$, $\eta^{(3)} = [\frac{d_3}{S_3}, 0]^T$, and $\eta^{(4)} = [\frac{d_4}{S_4}, 0]^T$. Then, an appropriate bound for the uncertainty functions $\eta^{(I)} \quad I = 1,2,3,4$ can be found as $\bar{\eta}^{(I)} \triangleq [\frac{\bar{d}_I}{S_I}, 0]^T$ where $\bar{d}_I = \bar{\gamma}_I\sqrt{2\mathcal{G}\mathcal{L}_I^{max}}$, $\bar{\gamma}_I$ is a constant threshold on γ_I, i.e., $\gamma_I(t) \le \bar{\gamma}_I \quad \forall t \ge 0$, and $\mathcal{L}_I^{max}$ denotes the maximum tank $\mathbb{T}_I$ level.

The nominal functions $p_i^{(I)}, \ i = 1,2, \ I = 1,2,3,4$ satisfy the Lipschitz condition for the function $p_i^{(I)}$ with Lipschitz constants $L_{p_i^{(I)}} = 0$ for all $i = 1,2, \ I = 1,2,3,4$. The interconnection functions $q_i^{(I)}, \ i = 1,2,$ satisfy the Lipschitz condition for the function $q_i^{(I)}$, and hence Lemma 4.1 with known constants $L_{q_1^{(I)}} = \frac{1}{S_I}$ and $L_{q_2^{(I)}} = 0$ for all $I = 1,2,3,4$. Therefore, the coefficient $L_i^{(I)} = L_{p_i^{(I)}} + L_{q_i^{(I)}}$ can be assigned as $L_1^{(I)} = \frac{1}{S_I}$ and $L_2^{(I)} = 0 \quad I = 1,2,3,4$. The unknown value opening $\gamma_I(t)$ are considered as $\gamma_1(t) = 2.5\sin(0.6t)$, $\gamma_2(t) = 2.5\sin(0.3t)$, $\gamma_3(t) = 2\sin(0.7t)$ and $\gamma_4(t) = 2\sin(2t)$. The inputs u_H are selected as

$$u_{H,1} = \begin{cases} 0.95 \text{ cm}^3/\text{s} & \text{If } y_1 < \mathcal{L}_1^{\ell} \quad \text{and} \quad u_{H,2} \ge 0.1 \\ 0.47 \text{ cm}^3/\text{s} & \text{If } y_1 < \mathcal{L}_1^{\ell} \quad \text{and} \quad u_{H,2} < 0.1 \\ 0 & \text{If } y_1 \ge \mathcal{L}_1^{\mathcal{U}}, \end{cases}$$

$$u_{H,2} = \begin{cases} 0.85 \text{ cm}^3/\text{s} & \text{If } y_3 < \mathcal{L}_2^{\ell} \quad \text{and} \quad u_{H,3} \ge 0.1 \\ 0.25 \text{ cm}^3/\text{s} & \text{If } y_3 < \mathcal{L}_2^{\ell} \quad \text{and} \quad u_{H,3} < 0.1 \\ 0 & \text{If } y_3 \ge \mathcal{L}_2^{\mathcal{U}}, \end{cases}$$

$$u_{H,3} = \begin{cases} 0.55 \text{ cm}^3/\text{s} & \text{If } y_5 < \mathcal{L}_3^{\ell} \quad \text{and} \quad u_{H,4} \ge 0.1 \\ 0.22 \text{ cm}^3/\text{s} & \text{If } y_5 < \mathcal{L}_3^{\ell} \quad \text{and} \quad u_{H,4} < 0.1 \\ 0 & \text{If } y_5 \ge \mathcal{L}_3^{\mathcal{U}}, \end{cases}$$

$$u_{H,4} = \begin{cases} 0.185 \text{ cm}^3/\text{s} & \text{If } y_7 \le \mathcal{L}_4^{\ell} \\ 0 \text{ cm}^3/\text{s} & \text{If } y_7 \ge \mathcal{L}_4^{\mathcal{U}}. \end{cases}$$

The actuators $u_{H,I} \quad I = 1,2,3,4$ values maintain their previous values outside the aforementioned intervals; for example, the actuator value $u_{H,1}$ when y_1 enters the interval $[\mathcal{L}_1^{\ell}, \mathcal{L}_1^{\mathcal{U}}]$ can be either 0 cm^3/s, 0.47 cm^3/s, 0.95 cm^3/s. The constants $\mathcal{L}_I^{\ell}$ and $\mathcal{L}_I^{\mathcal{U}}$ indicate the minimum and maximum level of the water in the Ith tank respectively. For safety reasons, the minimum operational capacity $\mathcal{L}_I^{\ell} \quad I = 1,2,3,4$ of tanks are respectively set at $\mathcal{L}_1^{\ell} = 20$ cm, $\mathcal{L}_2^{\ell} = 16$ cm, $\mathcal{L}_3^{\ell} = 16$ cm, and $\mathcal{L}_4^{\ell} = 15.9$ cm. In addition, the maximum operational capacity of tanks $\mathcal{L}_I^{\mathcal{U}} \quad I = 1,2,3,4$ are respectively set at $\mathcal{L}_1^{\mathcal{U}} = 30$ cm, $\mathcal{L}_2^{\mathcal{U}} = 30$ cm, $\mathcal{L}_3^{\mathcal{U}} = 22$ cm, and $\mathcal{L}_4^{\mathcal{U}} = 22.7$ cm. In this paper, AFI is investigated by considering the fault occurrence in actuator u_1 and u_2 at the same time $t = 5$ s, i.e., $T_{0,1} = 5$ s and $T_{0,2} = 5$ s. The other actuators u_3, and u_4 are considered as healthy. Considering the structure of actuator faults in this paper, which is given in Eq. (2), the parameters Λ_1 and Λ_2 are selected in a way to produce a different rate of actuator loss of effectiveness. Specifically, $\Lambda_1 = 0.8$ and $\Lambda_2 = 0.4$, to adjust the loss of effectiveness percentage respectively to 80% and 50% of the actuator value in the healthy condition and also, we consider $\delta_1 = 0.6$ and $\delta_2 = 0.5$. It is worth mentioning that when an input value $u_{H,i}^{(I)}$ is set to zero, then any fault in that actuator vanishes. It is worth noting that, we have considered positive-valued actuators in all simulations. As a result, in (30) we can not only confine the estimation of an actuator in $|\hat{u}_{F_I}^{(I)}| \le \mathcal{R}_{F_I}^{(I)}$, but another restriction for positive-valued actuators can be added as well, i.e., $\hat{u}_{F_I,i}^{(I)} \ge 0 \quad$ for all $i = 1, \ldots, m_I$ and $r = 1, \ldots, \mathcal{P}_I$. This is considered for estimation of the actuator u_1 and u_2 in simulations.

The parameters of the WaterSafe Testbed are as follows: the maximum tank level $\mathcal{L}_I^{max} = 50$ cm for $I = 1,2$ and $\mathcal{L}_I^{max} = 40$ cm for $I = 3,4$; the gravity constant $\mathcal{G} = 9.8\,\text{m}^2/\text{s}$; by considering the bounding functions $\bar{\gamma}_I(t) = 2.5 \quad I = 1,2$ and $\bar{\gamma}_I(t) = 2 \quad I = 3,4$, an appropriate bound for the unknown uncertainty can be calculated by

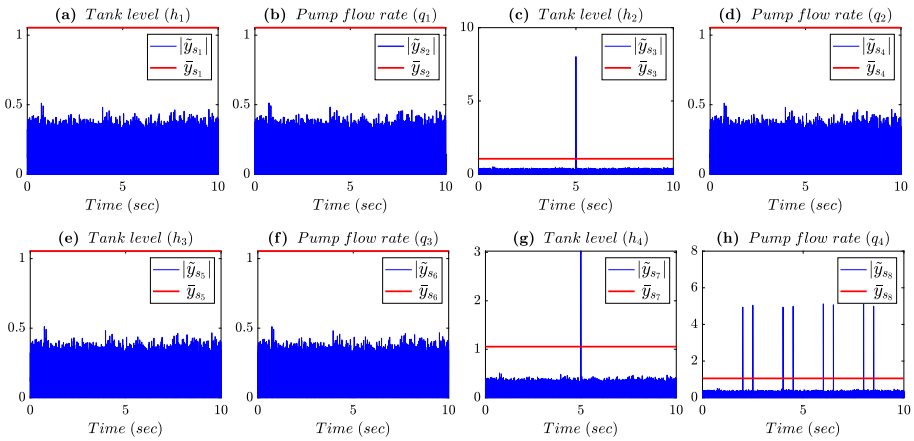

Fig. 7. Case A: sensor fault occurrence. The result of the SFI module, where the faulty sensors are y_3, y_5 and y_8, respectively with the faults $f_{y,3} = 8, f_{y,7} = 3$ and the intermittent fault as $f_{y,8} = 5 \quad t \in [2j, 2j + 0.5]$ for all $j = 1, 2, 3, \ldots$.

$d_I = \bar{\gamma}_I \sqrt{2\mathcal{G}\mathcal{L}_I^{max}} = 78.26 \quad I = 1, 2$ and $\bar{d}_I = 70 \quad I = 3, 4$; the tank diameter is 36 cm, then, the tank base area $S_I = \pi(\frac{36}{2})^2 \quad I = 1, 2, 3, 4$; the parameters of LFC in (46) are selected as $\alpha_I \triangleq 0.107, \lambda_I \triangleq 26.59$ and $\vartheta_I \triangleq -0.97$ for all $I = 1, 2, 3, 4$.

All simulations in this paper are performed considering the initial conditions $x(0) = [21, 0, 20, 0, 17, 0, 19, 0]$, and $\hat{x}(0) = y(0)$. The time-delay t_D for fault isolation is considered as $t_{D,i} = 0.1\,\text{s} \quad i = 1, 2, 3, 4$ and, as a result, the maximum change of faulty actuators is given in (33). The bound on actuator estimation error is defined as $\kappa_i(t) = u_{H,i}(t)e^{-(t-T_{d,i})} + 0.01 \quad i = 1, 2, 3, 4$.

In the AFI module, the estimator gain matrix $K^{(I)}$ are selected such that $K^{(I)}$ is diagonal and $A_k^{(I)} = A^{(I)} - K^{(I)}$ is Hurwitz and also as it was mentioned in (25), $A_k^{(I)} = diag\{a_{k,1}^{(I)}, \ldots, a_{k,n_I}^{(I)}\}$, must be selected such that $a_{k,i}^{(I)} + L_i^{(I)} < 0 \quad i = 1, \ldots, n_I$. To this end, the diagonal matrix $A_k^{(I)}$ are selected as $A_k^{(I)} = diag\{-2, -2\}$; and since $A^{(I)} = [0, \frac{1}{S_I}\,;\, 0, -\alpha_I]$, therefore, the estimator gain matrices $K^{(I)}$ are obtained as $K^{(I)} = [2, \frac{1}{S_I}\,;\, 0, 2 - \alpha_I]$ for all $I = 1, \ldots, 4$.

In the simulations, the sensor noise $\xi_{y,i}$ is considered Gaussian with zero mean and variance $\sigma^2_{\xi_{y_i}} = 9 \times 10^{-2}$ for all $i = 1, \ldots, 8$. Therefore, an appropriate bound for the sensor noise $\xi_{y,i}$ with this variance can be selected as $\bar{\xi}_{y,i} = 0.5266\,\text{cm}, \quad i = 1, \ldots, 8$ which is obtained as the maximum value from 10^{+8} random iterations. Furthermore, since $\xi_z^{(I)} = y_z^{(I)} - z^{(I)}$, the bound $\bar{\xi}_z^{(I)}$ can be determined by considering the value of its corresponding sensor noise threshold. Therefore, $\bar{\xi}_z^{(1)} \triangleq \bar{\xi}_{y,4}$, $\bar{\xi}_z^{(2)} \triangleq \bar{\xi}_{y,6}$, $\bar{\xi}_z^{(3)} \triangleq \bar{\xi}_{y,8}$, and also $\bar{\xi}_z^{(4)} \triangleq 0$, where $\bar{\xi}_{y,i}$ is the threshold value of the sensor noise $\xi_{y,i} \quad i = 1, \ldots, 8$.

(b) SFI decomposition procedure

Based on the decomposition procedure of the main system (1) performed for SFI, which is provided in (6), the WaterSafe Testbed system can be decomposed into 8 subsystems, in which each state dynamic $\dot{x}_i$ along with its sensor measurement y_i is considered as one subsystem $\Sigma_{s_i} \quad i = 1, \ldots, 8$. The dynamics representation of the SFI decomposition procedure can be similarly extracted from the AFI decomposition procedure for WaterSafe system given in (45). Then, the ith sensor isolation estimator $\hat{\Sigma}_{s_i} \quad i = 1, \ldots, 8$ is determined based on (8), where a diagonal estimator gain matrix $\mathcal{K}$ will be considered for the SFI task. In this paper, we have considered the SFI delay time $t_{0,1} = 0.1\text{s}$ and the discrepancy $\epsilon_1 = 5 \times 10^{-4}$. Hence, an optimal estimator gain obtained by utilizing part (b) of Theorem 3.1 will be $\mathcal{M}_{1\,1} = 400$. Note that the estimator gain $\mathcal{K}_{1\,1}$ has to be selected such that $\mathcal{K}_{1\,1} \geq \mathcal{M}_{1\,1}$ to fulfill the required accuracy, i.e, $|\tilde{y}_{s_1}(t)| \leq \bar{y}_{s_1}(t) \leq 2\bar{\xi}_{y,1} + \epsilon_1$. The same calculations can be performed for other sensor estimator gains as well. In the simulations, we have utilized the same estimator gain as $\mathcal{K}_{ii} = 1000$ for abrupt SFI of subsystem $\Sigma_{s_i} \quad i = 1, \ldots, 8$.

Simulation examples

In this paper, multiple sensor or actuator faults are considered in the system and the goal is to isolate them.

The simulation results are given by evaluating the designed scheme by considering the following two cases:

- Case A: sensor fault occurrence. The results of the SFI and AFI modules are given for the isolation of multiple faulty sensors in the system;
- Case B: actuator fault occurrence. The results of the SFI and AFI modules are given for the isolation of multiple faulty actuators in the system.

Case A: sensor fault occurrence.

In this case, multiple sensor fault occurrences are considered. Specifically, the sensors y_3 (i.e., y_{s_3}) and y_7 (i.e., y_{s_7}) become faulty respectively with the fault $f_{y,3} = 8$ and $f_{y,7} = 3$ at the same time $\mathcal{T}_{0,2} = 5\,\text{s}$. Furthermore, the sensor y_8 (i.e., y_{s_8}) is considered corrupted by an intermittent fault as $f_{y,8} = 5 \quad \forall t \in [2j, 2j + 0.5] \quad j = 1, 2, 3, \ldots$. The simulation results of the SFI module are given in Fig. 7. As it can be seen, the sensor faults in subsystems $\Sigma_{s_i} \quad i = 3, 7, 8$ are not only detected and isolated, since the faulty residuals exceed their corresponding thresholds but do not cause the violations of any other residuals. In other words, only residuals of the faulty sensors exceed their corresponding thresholds. Hence, considering the SFI theorem (Theorem 3.1), the faults in sensors y_3, y_5, and y_8 are accurately isolated as sensor faults.

It is worth noting that by isolating the faulty sensor components $y_i \quad i = 3, 7, 8$, the possibility of a diagnosed fault being an actuator fault will be excluded since we consider only a single fault type.

Fig. 8 depicts the results of the fault detection agent of the AFI module for all subsystems $\Sigma^{(I)} \quad I = 1, 2, 3, 4$ considering the Case A (multiple sensor fault occurrences), where only sensors y_3, y_7 and y_8 become faulty. As it can be seen, sensor faults are detected by the fault detection agents in the subsystems $\Sigma^{(I)} \quad I = 2, 4$ (sub-figures (c), (g) and (h)). As it was mentioned earlier, since a sensor fault has already been isolated by the SFI, the AFI results are overridden since we consider only a single fault type.

Case B: actuator fault occurrence.

In this case, actuators u_1 of subsystem $\Sigma^{(1)}$ and u_2 of subsystem $\Sigma^{(2)}$ become faulty simultaneously at time $T_{0,1}^{(I)} = 5\,\text{s} \quad I = 1, 2$.

In the sequel, the results of the SFI module and the AFI module for this case are demonstrated.

The simulation results of the SFI module for the subsystems $\Sigma_{s_i} \quad i = 1, 2, 3, 4$ (i.e., $\Sigma^{(1)}$ and $\Sigma^{(2)}$) are shown in Fig. 9(a)–(d). Note that due to page limitations, the results of subsystems $\Sigma_{s_i} \quad i = 5, \ldots, 8$ are

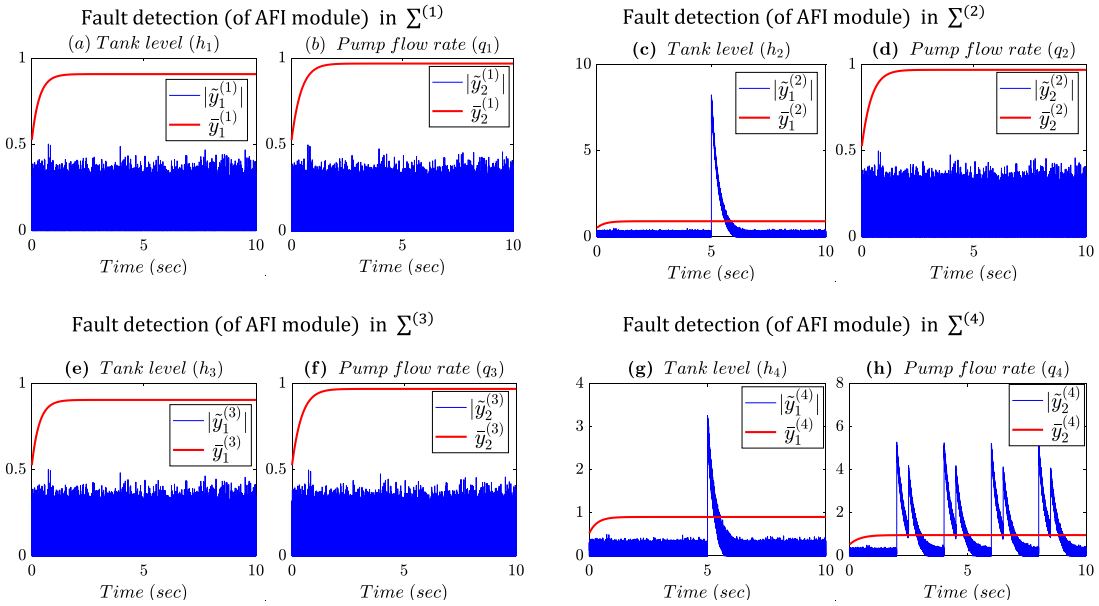

Fig. 8. Case A (sensor fault occurrence): the result of the fault detection in the AFI module, where the faulty sensors are y_3, y_5 and y_8, respectively with the faults $f_{y,3} = f^{(2)}_{y,1} = 8, f_{y,7} = f^{(4)}_{y,1} = 3$ and the intermittent fault as $f_{y,8} = f^{(4)}_{y,2} = 5 \quad t \in [2j, 2j + 0.5]$ for all $j = 1, 2, 3, \ldots$.

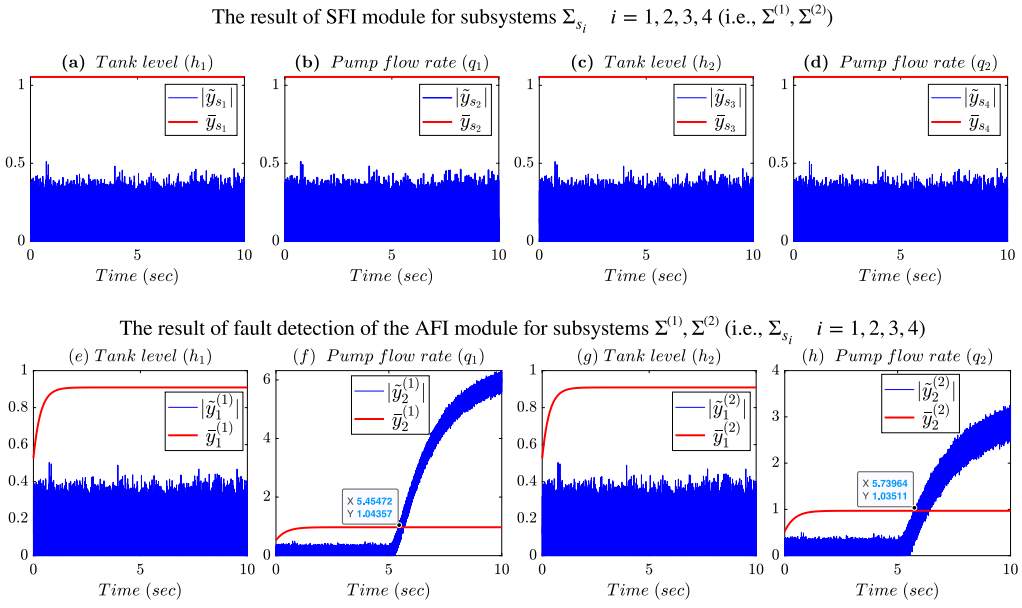

Fig. 9. Case B: actuator fault occurrence. The faulty actuators are u_1 and u_2 (i.e., $u^{(1)}_1$ and $u^{(2)}_1$). (a)–(d) the result of the SFI module, and (e)–(f) the results of the fault detection in the AFI module in $\Sigma^{(1)}, \Sigma^{(2)}$.

not shown. As it can be seen from Fig. 9, the actuator faults are not detected and not isolated by the SFI module, something that is in line with Theorem 3.1. Furthermore, the simulation results of the fault detection agent of the AFI modules are given in Fig. 9(e)–(h). As it can be seen, the residual $\tilde{y}^{(1)}_2$ in subsystem $\Sigma^{(1)}$ and the residual $\tilde{y}^{(2)}_2$ in subsystem $\Sigma^{(2)}$ exceed their corresponding detection thresholds $\bar{y}^{(1)}_2$ and $\bar{y}^{(2)}_2$ respectively, at times $T^{(1)}_d = 5.455\,\text{s}$ and $T^{(2)}_d = 5.739\,\text{s}$. The other subsystems $\Sigma^{(I)} \quad I = 3, 4$ do not detect any faults, but due to space constraints, these results are not shown.

Estimated residuals $\tilde{y}^{(1)}_{\mathcal{F}_{k_1},j} \quad j = 1, 2$ and their corresponding isolation thresholds $\bar{\bar{y}}^{(1)}_{\mathcal{F}_{k_1},j} \quad (\forall t > T^{(1)}_{d,j} + t^{(1)}_D)$ for the estimator $\hat{\Sigma}^{(1)}_{\mathcal{F}_1}$ are shown in Fig. 10(a)–(b). The faulty actuator $u^{(1)}_{\mathcal{F}_1}$ (i.e., u_1) and its adaptive estimation $\hat{u}^{(1)}_{\mathcal{F}_1}$ are given in Fig. 10(c). Similarly, the estimated residuals $\tilde{y}^{(2)}_{\mathcal{F}_{k_1},j} \quad j = 1, 2$ and their corresponding isolation thresholds $\bar{\bar{y}}^{(2)}_{\mathcal{F}_{k_1},j} \quad (\forall t > T^{(2)}_{d,j} + t^{(2)}_D)$ for the estimator $\hat{\Sigma}^{(2)}_{\mathcal{F}_1}$ are shown in Fig. 10(d)–(e). The faulty actuator $u^{(2)}_{\mathcal{F}_1}$ (i.e., u_2) and its adaptive estimation $\hat{u}^{(2)}_{\mathcal{F}_1}$ are given in Fig. 10(f). From this figure, especially from sub-figures (a)–(c), it can be inferred that the actuator $u^{(1)}_1$ is isolated as the faulty actuator in subsystem $\Sigma^{(1)}$, since the isolation residuals do not exceed their corresponding isolation thresholds. Similarly, from sub-figures (d)–(f), it can be inferred that the actuator $u^{(2)}_1$ is isolated as the faulty actuator in subsystem $\Sigma^{(2)}$. Finally, $\hat{u}^{(1)}_{\mathcal{F}_1}$ and $\hat{u}^{(2)}_{\mathcal{F}_1}$ can be considered as the estimations of the identified faulty actuators $u^{(1)}_1$ in subsystem $\Sigma^{(1)}$ and $u^{(2)}_1$ in subsystems $\Sigma^{(2)}$ respectively.

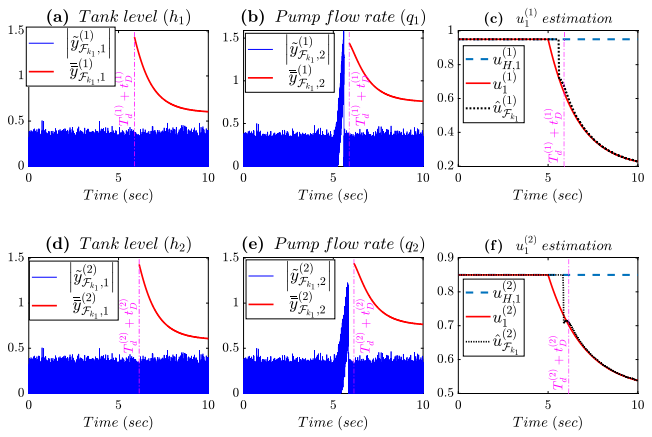

Fig. 10. Case B (actuator fault occurrence): the result of the adaptive approximation of actuator faults in the AFI module where (a)–(c) actuator $u_1^{(1)}$ estimation, and also (d)–(f) actuator $u_1^{(2)}$ estimation.

6. Conclusion

In this paper, we have presented a robust and unified fault isolation approach for effectively isolating multiple faulty actuators or sensors in a class of nonlinear dynamical systems. For sensor fault isolation, a modified Luenberger observer scheme has been designed, which provides simultaneous and accurate detection and isolation of multiple sensor faults, whilst remaining insensitive to faulty actuators in the system. The proposed SFI scheme guarantees accurate isolability of multiple potential sensor faults (even in the presence of multiple unknown actuator faults). In the case of AFI, an adaptive approximation scheme is designed to effectively isolate the actual set of faulty actuators. In this way, actuator fault isolation thresholds are designed to diagnose and distinguish the faulty actuators among all possible faulty actuator sets. Simulation results demonstrate the effective isolation of multiple actuator/sensor faults within a dynamical system through the developed AFI and SFI schemes. Actuator and sensor fault isolation in discrete-time nonlinear systems, communication limitations (event-triggered systems, input/output quantization), and utilizing the isolation information for accommodation purposes can be pursued as future work in this area.

CRediT authorship contribution statement

Hamed Tirandaz: Writing – review & editing, Writing – original draft, Methodology. **Christodoulos Keliris:** Writing – review & editing, Supervision, Methodology. **Marios M. Polycarpou:** Writing – review & editing, Supervision, Methodology, Funding acquisition.

Declaration of competing interest

The authors declare the following financial interests/personal relationships which may be considered as potential competing interests: Hamed Tirandaz, Christodoulos Keliris and Marios M. Polycarpou report financial support was provided by the European Research Council (ERC) under the ERC Synergy grant agreement No. 951424 (Water-Futures) and by the European Union's Horizon 2020 research and innovation programme under grant agreement No. 739551 (KIOS CoE) and the Government of the Republic of Cyprus through the Directorate General for European Programmes, Coordination and Development. Marios M. Polycarpou is an Advisory Board Member for *Journal of Automation and Intelligence* and was not involved in the editorial review or the decision to publish this article.

Data availability

No data was used for the research described in the article.

References

[1] R. Isermann, Fault-Diagnosis Systems: An Introduction from Fault Detection to Fault Tolerance, Springer Science & Business Media, 2005.
[2] I. Hwang, S. Kim, Y. Kim, C.E. Seah, A survey of fault detection, isolation, and reconfiguration methods, IEEE Trans. Control Syst. Technol. 18 (3) (2009) 636–653.
[3] M. Blanke, M. Kinnaert, J. Lunze, M. Staroswiecki, J. Schröder, third ed., Diagnosis and Fault-Tolerant Control, vol. 2, Springer, 2016.
[4] V. Reppa, M.M. Polycarpou, C.G. Panayiotou, Sensor fault diagnosis, Found. Trends Syst. Control 3 (1–2) (2016) 248.
[5] R. Rajamani, A. Ganguli, Sensor fault diagnostics for a class of non-linear systems using linear matrix inequalities, Internat. J. Control 77 (10) (2004) 920–930.
[6] S. Narasimhan, P. Vachhani, R. Rengaswamy, New nonlinear residual feedback observer for fault diagnosis in nonlinear systems, Automatica 44 (9) (2008) 2222–2229.
[7] H.A. Talebi, K. Khorasani, S. Tafazoli, A recurrent neural-network-based sensor and actuator fault detection and isolation for nonlinear systems with application to the satellite's attitude control subsystem, IEEE Trans. Neural Netw. 20 (1) (2009) 45–60.
[8] S. Rajaraman, J. Hahn, M.S. Mannan, Sensor fault diagnosis for nonlinear processes with parametric uncertainties, J. Hazard. Mater. 130 (1–2) (2006) 1–8.
[9] X. Zhang, T. Parisini, M.M. Polycarpou, Sensor bias fault isolation in a class of nonlinear systems, IEEE Trans. Automat. Control 50 (3) (2005) 370–376.
[10] J.M. Koscielny, M. Bartys, M. Ł Syfert, Method of multiple fault isolation in large scale systems, IEEE Trans. Control Syst. Technol. 20 (5) (2011) 1302–1310.
[11] V. Reppa, M.M. Polycarpou, C.G. Panayiotou, Decentralized isolation of multiple sensor faults in large-scale interconnected nonlinear systems, IEEE Trans. Automat. Control 60 (6) (2014) 1582–1596.
[12] X. Zhang, M.M. Polycarpou, T. Parisini, A robust detection and isolation scheme for abrupt and incipient faults in nonlinear systems, IEEE Trans. Automat. Control 47 (4) (2002) 576–593.
[13] C. Keliris, M.M. Polycarpou, T. Parisini, An integrated learning and filtering approach for fault diagnosis of a class of nonlinear dynamical systems, IEEE Trans. Neural Netw. Learn. Syst. 28 (4) (2017) 988–1004.
[14] A.B. Trunov, M.M. Polycarpou, Automated fault diagnosis in nonlinear multivariable systems using a learning methodology, IEEE Trans. Neural Netw. 11 (1) (2000) 91–101.
[15] H.A. Talebi, K. Khorasani, A neural network-based multiplicative actuator fault detection and isolation of nonlinear systems, IEEE Trans. Control Syst. Technol. 21 (3) (2012) 842–851.
[16] V. Reppa, M.M. Polycarpou, C.G. Panayiotou, Adaptive approximation for multiple sensor fault detection and isolation of nonlinear uncertain systems, IEEE Trans. Neural Netw. Learn. Syst. 25 (1) (2013) 137–153.
[17] X. Zhang, Sensor bias fault detection and isolation in a class of nonlinear uncertain systems using adaptive estimation, IEEE Trans. Automat. Control 56 (5) (2011) 1220–1226.
[18] X. Zhang, Q. Zhang, Distributed fault diagnosis in a class of interconnected nonlinear uncertain systems, Internat. J. Control 85 (11) (2012) 1644–1662.
[19] M.S. Phatak, N. Viswanadham, Actuator fault detection and isolation in linear systems, Internat. J. Systems Sci. 19 (1988) 2593–2603.
[20] W. Chen, M. Saif, An actuator fault isolation strategy for linear and nonlinear systems, in: Proceedings of the American Control Conference, IEEE, 2005, pp. 3321–3326.
[21] Z. Gao, S.X. Ding, Fault reconstruction for Lipschitz nonlinear descriptor systems via linear matrix inequality approach, Circuits Syst. Signal Process. 27 (3) (2008) 295–308.
[22] X. Zhang, M.M. Polycarpou, T. Parisini, Design and analysis of a fault isolation scheme for a class of uncertain nonlinear systems, Annu. Rev. Control 32 (1) (2008) 107–121.
[23] M. Du, J. Scott, P. Mhaskar, Actuator and sensor fault isolation of nonlinear process systems, Chem. Eng. Sci. 104 (2013) 294–303.
[24] J.W. Zhu, G.H. Yang, H. Wang, F. Wang, Fault estimation for a class of nonlinear systems based on intermediate estimator, IEEE Trans. Automat. Control 61 (9) (2015) 2518–2524.
[25] Y. Wu, B. Jiang, N. Lu, A descriptor system approach for estimation of incipient faults with application to high-speed railway traction devices, IEEE Trans. Syst. Man Cybern. Syst. 49 (10) (2019) 2108–2118.
[26] L. Chen, S. Fu, Y. Zhao, M. Liu, J. Qiu, State and fault observer design for switched systems via an adaptive fuzzy approach, IEEE Trans. Fuzzy Syst. 28 (9) (2019) 2107–2118.
[27] L. Chen, M. Liu, Y. Shi, H. Zhang, E. Zhao, Adaptive fault estimation for unmanned surface vessels with a neural network observer approach, IEEE Trans. Circuits Syst. I. Regul. Pap. 68 (1) (2020) 416–425.
[28] C. Keliris, M.M. Polycarpou, T. Parisini, Distributed fault diagnosis for process and sensor faults in a class of interconnected input–output nonlinear discrete-time systems, Internat. J. Control 88 (8) (2015) 1472–1489.
[29] S. Gentil, J. Montmain, C. Combastel, Combining FDI and AI approaches within causal-model-based diagnosis, IEEE Trans. Syst. Man Cybern. B 34 (5) (2004) 2207–2221.

[30] W. Zhang, S. Shen, Z. Han, Sufficient conditions for hurwitz stability of matrices, Lat. Amer. Appl. Res. 38 (3) (2008) 253–258.
[31] P.A. Ioannou, J. Sun, Robust Adaptive Control, Prentice-Hall, Englewood Cliffs, NJ, USA, 1995.
[32] C. Keliris, A Filtering Approach for Fault Diagnosis of Nonlinear Uncertain Systems (Ph.D. thesis), University of Cyprus, 2015.
[33] C. Keliris, M.M. Polycarpou, T. Parisini, A distributed fault detection filtering approach for a class of interconnected continuous-time nonlinear systems, IEEE Trans. Automat. Control 58 (8) (2013) 2032–2047.
[34] V. Reppa, M.M. Polycarpou, C.G. Panayiotou, Multiple sensor fault detection and isolation for large-scale interconnected nonlinear systems, in: 2013 European Control Conference, ECC, IEEE, 2013, pp. 1952–1957.
[35] R.J. Patton, P.M. Frank, R.N. Clarke, Fault Diagnosis in Dynamic Systems: Theory and Application, Prentice-Hall, Inc., 1989.
[36] M.M. Polycarpou, A.J. Helmicki, Automated fault detection and accommodation: a learning systems approach, IEEE Trans. Syst. Man Cybern. 25 (11) (1995) 1447–1458.
[37] P. Mhaskar, C. McFall, A. Gani, P.D. Christofides, J.F. Davis, Isolation and handling of actuator faults in nonlinear systems, Automatica 44 (1) (2008) 53–62.
[38] J.A. Farrell, M.M. Polycarpou, Adaptive Approximation Based Control: Unifying Neural Fuzzy and Traditional Adaptive Approximation Approaches, John Wiley & Sons, 2006.
[39] M.M. Polycarpou, A.T. Vemuri, Learning methodology for failure detection and accommodation, IEEE Control Syst. Mag. 15 (3) (1995) 16–24.
[40] S. Vrachimis, S. Santra, A. Agathokleous, P. Pavlou, M. Kyriakou, M. Psaras, D.G. Eliades, M.M. Polycarpou, Watersafe: A water network benchmark for fault diagnosis research, IFAC-PapersOnLine 55 (6) (2022) 655–660.

Hamed Tirandaz holds a B.Sc. in Applied Mathematics from Hakim Sabzevari University, awarded in 2006, and an M.Sc. in Mechatronics Engineering from Semnan University, Iran, completed in 2009. Subsequently, he ventured into the software industry, where he worked as a programmer for a power distribution system company. From 2010 to 2019, he served as a Lecturer at Hakim Sabzevari University, Sabzevar, Iran. Currently, he is dedicated to his Ph.D. studies at the Department of Electrical and Computer Engineering at the University of Cyprus, and researcher at the KIOS Center of Excellence. His research interests primarily focus around fault diagnosis, and fault-tolerant control of distributed systems.

Christodoulos Keliris received the Diploma (Hons.) degree in electrical and computer engineering from the Aristotle University of Thessaloniki, Greece, in 2007, the M.Sc. (Hons.) degree in finance from Imperial College London, UK in 2008, and the Ph.D. degree in electrical engineering from the University of Cyprus, Cyprus, in 2015. He was a Researcher in various European research and operational programmes. His current research interests include fault diagnosis for nonlinear systems, nonlinear control theory, adaptive learning, intelligent systems, and security of cyber–physical systems.

Dr. Keliris is a Reviewer for various conferences and journals. His dissertation Pricing Barrier Options received the Best M.Sc. Finance Dissertation Prize.

Marios M. Polycarpou is a Professor of Electrical and Computer Engineering and the Director of the KIOS Research and Innovation Center of Excellence at the University of Cyprus. He is also a Founding Member of the Cyprus Academy of Sciences, Letters, and Arts, an Honorary Professor of Imperial College London, and a Member of Academia Europaea (The Academy of Europe). He received the B.A degree in Computer Science and the B.Sc. in Electrical Engineering, both from Rice University, USA in 1987, and the M.S. and Ph.D. degrees in Electrical Engineering from the University of Southern California, in 1989 and 1992 respectively. His teaching and research interests are in intelligent systems and networks, adaptive and learning control systems, fault diagnosis, machine learning, and critical infrastructure systems.

Prof. Polycarpou is the recipient of the *2023 IEEE Frank Rosenblatt Technical Field Award* and the 2016 *IEEE Neural Networks Pioneer Award*. He is a Fellow of IEEE and IFAC. He served as the President of the IEEE Computational Intelligence Society (2012–2013), as the President of the European Control Association (2017–2019), and as the Editor-in-Chief of the *IEEE Transactions on Neural Networks and Learning Systems (2004–2010)*. Prof. Polycarpou currently serves on the Editorial Boards of the *Proceedings of the IEEE* and the *Annual Reviews in Control*. His research work has been funded by several agencies and industry in Europe and the United States, including the prestigious European Research Council (ERC) Advanced Grant, the ERC Synergy Grant and the EU-Widening Teaming program.